WFDE5: bias adjusted ERA5 reanalysis data for impact studies

Marco Cucchi[1], Graham P. Weedon[2], Alessandro Amici[1], Nicolas Bellouin[3], Stefan Lange[4],
Hannes Müller Schmied[5,6], Hans Hersbach[7], and Carlo Buontempo[7]

[1]B-Open Solutions srl, Rome, Italy
[2]Met Office, Maclean Building, Benson Lane, Crowmarsh Gifford, Wallingford, Oxfordshire, OX10 8BB, United Kingdom
[3]Department of Meteorology, University of Reading, Reading, RG6 6BB, United Kingdom
[4]Potsdam Institute for Climate Impact Research (PIK), Member of the Leibniz Association, P.O. Box 60 12 03, 14412 Potsdam, Germany
[5]Institute of Physical Geography, Goethe University Frankfurt, Frankfurt am Main, Germany
[6]Senckenberg Leibniz Biodiversity and Climate Research Centre (SBiK-F), Frankfurt am Main, Germany
[7]European Centre for Medium-Range Weather Forecasts, Reading, United Kingdom

Correspondence: Carlo Buontempo (carlo.buontempo@ecmwf.int)

Abstract. The WFDE5 dataset has been generated using the WATCH Forcing Data (WFD) methodology applied to surface meteorological variables from the ERA5 reanalysis. The WFDEI dataset had previously been generated by applying the WFD methodology to ERA-Interim. The WFDE5 is provided at 0.5° spatial resolution, but has higher temporal resolution (hourly) compared to WFDEI (3-hourly). It also has higher spatial variability since it was generated by aggregation of the higher-resolution ERA5 rather than by interpolation of the lower resolution ERA-Interim data. Evaluation against meteorological observations at 13 globally distributed FLUXNET2015 sites shows that, on average, WFDE5 has lower mean absolute error and higher correlation than WFDEI for all variables. Bias-adjusted monthly precipitation totals of WFDE5 result in more plausible global hydrological water balance components as analyzed in an uncalibrated hydrological model (WaterGAP) than use of raw ERA5 data for model forcing.

The dataset, which can be downloaded from https://doi.org/10.24381/cds.20d54e34 (C3S, 2020), is distributed by the Copernicus Climate Change Service (C3S) through its Climate Data Store (CDS, C3S, 2020) and currently spans from the start of January 1979 to the end of 2018. The dataset has been produced using a number of CDS Toolbox applications, whose source code is available with the data - allowing users to re-generate part of the dataset or apply the same approach on other data. Future updates are expected spanning from 1950 to the most recent year.

A sample of the complete dataset, which covers the whole 2016 year, is accessible without registration to the CDS at https://doi.org/10.21957/935p-cj60.

1 Introduction

The development, calibration and evaluation of impact models requires good quality historical meteorological datasets. These are needed to both drive the impact models themselves and characterise their performances over the historical period. The availability of reliable historical runs is also critical for the preparation of impact studies using climate projections. Reanalyses have long been used for those purposes as they provide a physically consistent global reconstruction of past weather without any gap in space or in time. The ERA-Interim global reanalysis for the atmosphere, land surface and ocean waves (Dee et al., 2011) of the European Centre for Medium Range Weather Forecast (ECMWF) has been used widely as a reference by the climate community. Although reanalyses represent -by construction- the most plausible state of the atmosphere and the ocean given the observations and the forecasts from the model at a previous time-step, the coarse resolutions of models, the assumptions made in sub-grid parameterisations, and more generally the overall inadequacies of the modelling framework, are known to induce biases with respect to ground-based observations and radiosondes. Considering that the primary goal of impact studies is to assess the climate change impacts in the real world (as opposite to the model world) it is essential that such biases are first characterised and then, as much as practically possible, corrected for.

Recently the ERA5 reanalysis has superseded the ERA-Interim reanalysis (Hersbach et al., 2020). It is produced at ECMWF as part of the EU-funded Copernicus Climate Change Service (C3S). At the time of writing data was available from the C3S Climate Data Store (CDS) for the period from 1979 onwards. Timely updates are provided with a 5-day latency, while a more thorough quality check is provided 2-3 months later. In 2020 the dataset will be extended back to 1950, and will then also encompass the period covered by ERA-40 (1957–2002; Uppala et al., 2005). ERA5 is based on 4D-Var data assimilation using Cycle 41r2 of the Integrated Forecasting System (IFS), which was operational at ECMWF in 2016. As such, compared to ERA-Interim (which was based on an IFS cycle that dates from 2006) ERA5 benefits from a decade of developments in model physics, core dynamics and data assimilation. In addition to a significantly enhanced horizontal resolution (31 km grid spacing compared to 80 km for ERA-Interim), ERA5 has a number of innovative features. These include hourly output throughout and an uncertainty estimate. The uncertainty information is obtained from a 10-member ensemble of data assimilations with 3-hourly output at half the horizontal resolution (63 km grid spacing). Compared to ERA-Interim, ERA5 also provides an enhanced number of output parameters. An overview of the main characteristics and general performance of ERA5 and a comparison with ERA-Interim is provided in Hersbach et al. (2020), while more in-depth studies of particular aspects have been reported in a growing number of publications in the scientific literature.

The move from ERA-Interim to ERA5 represents a step change in overall quality and level of detail, whose increase has been reported in a large number of publications. Several of these have been summarized in Hersbach et al. (2020), and the benefit of hourly resolution is illustrated for the December 1999 storm Lothar in that paper as well. Hersbach et al. (2019) shows the increased level in detail of precipitation over the North Atlantic.

ERA5 utilizes a vast amount of synoptic observations. The number has increased from approximately 0.75 million per day on average in 1979 to around 24 million per day by the end of 2018. Satellite radiances are the dominant and growing type of data throughout the period. The volume of conventional data has also increased steadily. In addition to observations, ERA5

relies on gridded information about radiative forcing and boundary conditions. For radiation, ERA5 includes forcings for total solar irradiance, ozone, greenhouse gases and some aerosols developed for the World Climate Research Programme (WCRP) Coupled Model Intercomparison Project Phase 5 (CMIP5) initiative, including stratospheric sulphate aerosols. This represents a major improvement on ERA-Interim, which, for example, does not account for stratospheric sulphate aerosols due to major volcanic eruptions. Details are provided in Hersbach et al. (2015). The evolution of sea-surface temperature (SST) and sea ice cover is based on a combination of products: the UK Met Office Hadley Centre HadISST2 product for SST, the EUMETSAT OSI-SAF reprocessed product for sea ice, and the UK Met Office OSTIA product for SST and sea ice that is also used in ECMWF's operational forecasting system. Details can be found in Hirahara et al. (2016).

The EU WATCH programme produced a common framework for land surface models (LSMs) and global hydrological models (GHMs) to assess the global terrestrial hydrological cycle in the 20th & 21st centuries. This required a common meteorological forcing dataset for the 20th century which became the WATCH Forcing Data (WFD). The WFD, based on the ERA40 reanalysis, allowed intercomparisons of hydrological models and bias correction of 21st century GCM outputs (Haddeland et al., 2011; Hagemann et al., 2011). The modelling in WATCH required sub-daily, and daily average data, at half-degree spatial resolution necessitating interpolation onto the regular latitude-longitude grid, land-sea mask and elevations used by the Climate Research Unit (CRU). The WFD methodology (Weedon et al., 2010, 2011) involved common processing of all terrestrial half-degree grid boxes outside Antarctica at three hourly steps, with elevation correction of air temperature and consequent adjustment of surface pressure, specific humidity and downwards longwave radiation. Bias correction utilized the CRU gridded observations (New et al., 1999, 2000) of monthly average air temperature, diurnal temperature range, cloud cover (for adjusting average downwards shortwave fluxes), precipitation totals and number of "wet" (i.e. precipitation) days. Additionally, downwards shortwave radiation was corrected for changes in multi-year tropospheric and stratospheric aerosol loading. Unlike most other reanalyses ERA provides rainfall and snowfall rates separately and this permitted adjustment of these rates to allow for the precipitation gauge catch corrections inherent in the observed CRU precipitation totals. Though critical for hydrological modelling, the precipitation variables are the least well constrained by surface observations, so data were provided in two versions dependent on the source of the gridded monthly observed precipitation totals – one based on CRU and the other on the "full data product" of the Global Precipitation Climatology Centre (GPCC).

Later the WFD methodology was applied to the ERA-Interim reanalysis (Dee et al., 2011) to produce the WFDEI dataset (Weedon et al., 2014). As before the reanalysis data were 3-hourly and interpolated onto the CRU land-sea mask. Unlike the WFD, the WFDEI includes Antarctica and an extra processing step was introduced for the precipitation variables after correction of monthly totals and numbers of wet days, and before correction of precipitation gauge biases. This involved overriding the reanalysis ratio of rainfall to snowfall in each time step in cases where the differences between the CRU grid box elevation differed substantially from ERA-Interim elevation (Weedon et al., 2014). Intermittent updates of the WFDEI beyond 2009 used the latest versions of CRU and GPCC – i.e. WFDEI files for additional years were added rather than entire new versions of the files created.

Here we describe the WFDE5 (i.e. "WATCH Forcing Data methodology applied to ERA5 reanalysis data", C3S, 2020), a new meteorological forcing dataset for land surface and hydrological models based on the ERA5 reanalysis (Copernicus

Table 1. Sources of data used to derive the WFDE5 dataset

Dataset	Summary	Location
ERA5	ECMWF reanalysis product	https://cds.climate.copernicus.eu/cdsapp#!/home
CRU TS4.03	Climate Research Unit gridded station observations (multiple variables)	http://data.ceda.ac.uk/badc/cru/data/cru_ts/cru_ts_4.03
GPCCv2018	Global Precipitation Climatology Centre gridded station precipitation observations	https://opendata.dwd.de/climate_environment/GPCC/html/fulldata-monthly_v2018_doi_download.html

Climate Change Service, 2017). It consists of eleven variables (see Table 2) with an hourly temporal resolution on a regular longitude-latitude half-degree grid, with global spatial coverage and values defined only for land and lake points. The dataset was derived by applying the sequential elevation and monthly bias correction methods described in Weedon et al. (2010, 2011) to half-degree aggregated ERA5 reanalysis products. The monthly observational datasets used for bias correction are CRU TS4.03 from CRU (Harris et al., 2020) for 1979 to 2018 for all variables and the GPCCv2018 full data product (Schneider et al., 2018) for rainfall and snowfall rates for 1979 to 2016. In addition, as described below, the aerosol correction step for shortwave radiation has been revised with respect to WFD and WFDEI. For an outline of the methodology applied and a reference to the observation datasets used see Tables 1 and 2.

As a meteorological forcing dataset, WFDE5 facilitates climate impact simulations such as those carried out in the Inter-Sectoral Impact Model Intercomparison Project (ISIMIP; Warszawski et al., 2014; Frieler et al., 2017). It can be used to directly drive historical impact simulations, which are needed for impact model validation. It can also be used as an observational reference dataset for the bias adjustment of future climate projections; these bias-adjusted climate projections can then be used to drive future climate impact projections. Both predecessors of WFDE5 have been employed for these two purposes in previous ISIMIP phases. In particular, the bias adjustment of future climate projections was done using the WFD in the ISIMIP Fast Track (Hempel et al., 2013) and the EartH2Observe, WFDEI and ERA-Interim data Merged and Bias-corrected for ISIMIP (EWEMBI; Lange, 2018, 2019a) in ISIMIP2b (Frieler et al., 2017). WFDE5 will be similarly employed in the upcoming ISIMIP phase 3.

2 Dataset Processing

All computations were carried out within the CDS Toolbox, a python coding environment to retrieve, process, plot and download data from the C3S Climate Data Store (CDS, C3S, 2020). The CDS Toolbox scripts used to generate the dataset are publicly available at https://doi.org/10.24381/cds.20d54e34 under a free and open licence, and can be used to reproduced the dataset.

Table 2. WFDE5 elevation and bias correction methodology outline (Weedon et al., 2010, 2011)

Variable name	Description	Units	Time step adjustments	Data used for monthly bias correction
Wind	10 m wind speed	$m\ s^{-1}$	Nil	Nil
Tair	2 m air temperature	K	Via environmental lapse rate	CRU TS4.03 temperature and diurnal temperature range
PSurf	Pressure at the surface	Pa	Via changes in Tair	Nil
Qair	2 m specific humidity	$kg\ kg^{-1}$	Via changes in Tair and PSurf	Nil
LWdown	Downward longwave radiation flux	$W\ m^{-2}$	Via fixed relative humidity and changes in Tair, PSurf, and Qair	Nil
SWdown	Downward shortwave radiation flux	$W\ m^{-2}$	Nil	CRU TS4.03 cloud cover and effects of interannual changes in atmospheric aerosol loading
Rainf [(CRU)]	Rainfall rate	$kg\ m^{-2}\ s^{-1}$	Adjustment of snow/rainfall ratios	CRU TS4.03 number of wet days, CRU TS4.03 precipitation totals, ERA5 ratio of rainfall/precipitation, rainfall gauge correction
Snowf [(CRU)]	Snowfall rate	$kg\ m^{-2}\ s^{-1}$	Adjustment of snow/rainfall ratios	CRU TS4.03 number of wet days, CRU TS4.03 precipitation totals, ERA5 ratio of rainfall/precipitation, snowfall gauge correction
Rainf [(CRU+GPCC)]	Rainfall rate	$kg\ m^{-2}\ s^{-1}$	Adjustment of snow/rainfall ratios	CRU TS4.03 number of wet days, GPCCv2018 precipitation totals, ERA5 ratio of rainfall/precipitation, rainfall gauge correction
Snowf [(CRU+GPCC)]	Snowfall rate	$kg\ m^{-2}\ s^{-1}$	Adjustment of snow/rainfall ratios	CRU TS4.03 number of wet days, GPCCv2018 precipitation totals, ERA5 ratio of rainfall/precipitation, snowfall gauge correction
ASurf	Grid-points altitude	m	Nil	Nil

NOTE: Variable names and units are based on the ALMA (Assistance for Land-surface Modeling Activities) conventions (http://www.lmd.jussieu.fr/ polcher/ALMA/); Wind, Tair, PSurf and Qair variables have instantaneous values, while LWdown, SWdown, Rainf and Snowf have average over the next hour at each date-time.

2.1 Extraction and aggregation of reanalysis data

ERA5 reanalysis data are available in the CDS on regular latitude-longitude grids at $0.25° \times 0.25°$, as a result of finite element-based linear interpolation from the original reduced Gaussian grid at $\sim 0.28°$, and atmospheric parameters are distributed on 37 pressure levels. They are distributed at hourly resolution, and the date and time to which each value refers to is represented using the validity date/time: for instantaneous variables, it corresponds to the date and time at which each value is considered valid; for accumulated variables, it represents the ending date and time of the interval over which the variable is accumulated, and hence over which each value can be considered valid. Accumulation variables are aggregated over the hour ending at the validity date/time, and they are automatically converted to mean rates when retrieved from within the CDS Toolbox.

Before applying elevation and bias correction, two preprocessing steps were performed on ERA5 reanalysis data. First, in order to enable comparison and bias correction using the CRU dataset, ERA5 reanalysis were regridded to regular half-degree longitude-latitude grid, via first-order conservative remapping (Jones, 1999). Then, a backward one-hour time shift was applied to rate variables, so that values stored at each date-time represents time averages over the following hour. The latter step was taken in order to adhere to the scheme used for the WATCH Forcing Dataset (Weedon et al., 2011).

It is worth noticing that grid-points classified as belonging to land in CRU TS4.03 and GPCCv2018 datasets are not necessarily classified as land-points in ERA5 reanalysis dataset. This is especially true for coastal grid-points, for which not considering this issue often led to anomalous values in the first iteration of the WFDE5 dataset. For this reason, besides applying CRU TS4.03/GPCCv2018 to ERA5 reanalysis after half-degree regridding, an additional mask derived by ERA5 quarter-degree land-sea and lake cover mask is applied just after retrieval. In this way, the final WFDE5 dataset contains values only for grid-points which are classified as land or lake by both ERA5 and CRU.

2.2 Elevation and bias correction

Once aggregation had been performed, the sequential elevation and monthly bias correction methods of Weedon et al. (2010, 2011) were applied to the regridded data (see Table 2). The same procedures used for the creation of the WFDEI (Weedon et al., 2014) were applied, with the only exception of near-surface specific humidity (Qair). For this variable, given the absence of both ERA5 near-surface specific and relative humidity from the CDS, a slightly different approach was taken: first, ERA5 vapor pressure and saturation vapor pressure at the surface, e and e_{sat} respectively, were computed following Buck (1981); then, they were used to compute ERA5 relative humidity at surface as $RH = 100.0 \cdot e/e_{sat}$; finally, at this point, the algorithm described in Weedon et al. (2010) could be resumed.

Likewise for the WFD (Weedon et al., 2011) and WFDEI (Weedon et al., 2014) datasets, downward shortwave radiation was adjusted at the monthly time scale using CRU cloud cover and the local linear correlation between monthly average (aggregated) ERA5 cloud cover and downward shortwave radiation (Sheffield et al., 2006; Weedon et al., 2010).

ERA5 includes a simplified representation of the time evolution of sulfate aerosols, which interact with radiation only in that model, but otherwise does not account for the impact on surface radiative fluxes of changes in aerosol interactions with radiation (also called direct effects of aerosols) and clouds (also called first indirect effects of aerosols). To represent those

impacts, aerosol corrections are calculated as monthly distributions of the anomaly in downward surface shortwave radiative flux due to aerosol-radiation and aerosol-cloud interactions over the period 1979-2018. Radiative transfer calculations, which use the tools described in section 2.f.ii of Weedon et al. (2010), are based on monthly-averaged distributions of tropospheric and stratospheric aerosol optical depth, and cloud fraction. The time series of tropospheric optical depth for sulfate, fossil-fuel black and organic carbon, biomass burning, mineral dust, seasalt, and secondary biogenic aerosols is taken from the historical and RCP8.5 simulations by the HadGEM2-ES climate model (Bellouin et al., 2011). To correct for biases in HadGEM2-ES aerosol optical depths, these optical depths are scaled over the whole period and for each aerosol species to match the global and monthly averages obtained by the CAMS Reanalysis of atmospheric composition (2003-2017; Inness et al. (2019)), which assimilates satellite retrievals of aerosol optical depth. This bias correction was not applied in WFD and WFDEI but is now possible thanks to the availability of the CAMS Reanalysis. The time series of stratospheric aerosol optical depth is taken from the climatology by Sato et al. (1993), which has been updated to 2012 at data.giss.nasa.gov/modelforce/strataer/. Years 2013-2017 are assumed to match background years so they replicate year 2010. That assumption is supported by the Global Space-based Stratospheric Aerosol Climatology time series (1979-2016; Thomason et al., 2018). The time series of cloud fraction is taken from CRU TS 4.03, for consistency with other aspects of the WFDE5 dataset. Surface radiative fluxes account for aerosol-radiation interactions from both tropospheric and stratospheric aerosols, and for aerosol-cloud interactions from tropospheric aerosols, except mineral dust. The radiative effects of aerosol-cloud interactions are assumed to scale with the radiative effects of aerosol-radiation interactions, using regional scaling factors derived from HadGEM2-ES. To avoid double-counting the radiative effects of aerosol-radiation interactions by sulfate aerosols, which are to some extent already represented in ERA5, the radiative transfer calculations are repeated, this time only including sulfate aerosol-radiation interactions, and the corresponding anomalies subtracted from the set of fluxes obtained previously. Atmospheric constituents other than aerosols and clouds are set to a constant standard mid-latitude summer atmosphere, because their variations only have second-order effects on aerosol corrections.

Finally, similarly to the WFD and WFDEI datasets, two different WFDE5 rainfall and snowfall rates datasets, including gauge catch corrections, were generated by using either CRU TS4.03 or GPCCv2018 precipitation totals. The GPCCv2018 database includes around 3–4 times as many precipitation stations as CRU (incorporating most of the latter as a subset (Becker et al., 2013; Schneider et al., 2014)), but extends only till 2016. As already pointed out in Weedon et al. (2014), during generation of the WFDE5 precipitation rates an error in the precipitation phase can arise locally where there are large elevation differences between ERA5 and CRU grids. For this reason, a further processing step was added to the WFD methodology to correct the most extreme cases of inappropriate precipitation phase: for each grid box and each calendar month over 1979–2018, records of the minimum Tair during rainfall and the maximum Tair during snowfall ("phase temperature extremes") were stored; then, for each grid box and hourly time step, the precipitation phase was switched if the combination of the phase with the elevation and bias-corrected Tair were beyond a phase temperature extreme.

Elevation and bias correction was applied for all land points outside Antarctica. For grid points belonging to this region, given the absence of observational data, only elevation correction was applied.

2.3 Higher resolution WFDE5 data

The WFDE5 has been provided at $0.5° \times 0.5°$ resolution rather than at $0.25° \times 0.25°$ as in the original ERA5 data. There are several reasons for this. The project to generate WFDE5 was designed also to deliver open source software so that users could re-generate the data at the original or, eventually, higher resolution. Three main considerations influenced the initial generation of the WFDE5 dataset:

1. The need to generate data in time for ISIMIP3 and their reporting to the AR6 of IPCC in 2020;

2. The need to convert the existing WFDEI Fortran programs into CDS Toolbox workflows and easily test the output;

3. The requirement for appropriate, and freely-available, global land gridded observations for bias correction.

The first consideration meant that any procedures adopted had to be practical and fast. The simplest way to test whether the CDS Toolbox workflows programs were working was to apply them to ERA-Interim data and check that they correctly reproduced the WFDEI data. This implied generating output at the same resolution as the WFDEI and CRU. Additionally, ISIMIP3 only required data at $0.5° \times 0.5°$ since their models were set up at that resolution.

The WFDE5 CDS workflows will eventually allow users to generate higher resolution data on their own. At the moment, this can only be done using interpolated CRU TS4.03 and GPCCv2018 datasets, copies of which are hosted on a dedicated CDS machine and made accessible through the CDS Toolbox. Another option would be to use higher-resolution observational datasets, such as quarter-degree GPCC or MSWEP (Beck et al., 2017, 2019b) for total precipitation. This option will be viable once additional datasets can be hosted on the C3S Climate Data Store.

3 Code and data availability

The WFDE5 dataset is distributed by the Copernicus Climate Change Service (C3S) through its Climate Data Store (CDS) as monthly files in NetCDF format, and can be downloaded at https://doi.org/10.24381/cds.20d54e34 (C3S, 2020). It uses a full half-degree grid (720×360 grid boxes) with the sea/large lakes flagged as missing data, comprising a total of 92889 land points (Antarctica included). General dataset attributes are described in Table 3. A sample of the complete dataset, which covers the whole 2016 year, is accessible without registration to the CDS at https://doi.org/10.21957/935p-cj60.

All the CDS Toolbox workflows used to generate WFDE5 are publicly available https://doi.org/10.24381/cds.20d54e34, and can be used to re-generate samples of the dataset. Furthermore, as ERA5 progresses, using these applications it will be possible to expand WFDE5 dataset back to the start of 1950 and forward beyond 2018.

Table 3. Summary of WFDE5 dataset attributes on the C3S Climate Data Store

Dataset attribute	Details
Horizontal coverage	Global
Horizontal resolution	0.5° x 0.5°
Vertical coverage	Surface
Temporal coverage	- 1979-01-01 00:00:00 to 2018-12-31 23:00:00 for variables Wind, Tair, PSurf and Qair - 1979-01-01 07:00:00 to 2018-12-31 23:00:00 for variables LWdown, SWdown, Rainf $^{(CRU)}$, Snowf $^{(CRU)}$ - 1979-01-01 07:00:00 to 2016-12-31 23:00:00 for variables Rainf $^{(CRU+GPCC)}$, Snowf $^{(CRU+GPCC)}$
Temporal resolution	Hourly
File format	NetCDF
Data type	Grid
Version	1.0
File naming convention	`<var>_WFDE5_<reference_dataset>_<YYYYMM>_v1.0.nc`, where - `<var>`: variable name, as in Table 2 - `<reference_dataset>`: one between CRU (all variables) and CRU+GPCC (Rainf and Snowf only) - `<YYYYMM>`: year and month

4 Evaluation

4.1 Previous analyses

Beck et al. (2019a) assessed multiple precipitation datasets at daily time steps against radar and precipitation gauge observations across the co-terminus USA. Their analysis included ERA5, ERA-Interim and WFDEI precipitation adjusted to GPCC totals. They demonstrated that against observations ERA5 precipitation provides a significant improvement over both ERA-Interim and WFDEI precipitation. Albergel et al. (2018) used the ISBA LSM to assess the use of ERA5 versus ERA-Interim forcing. They assessed performance against a wide variety of observed hydrological and vegetation-related variables. Significant improvements were demonstrated in simulation of the hydrological cycle using ERA5 which they mostly attributed to better precipitation. There were small changes related to vegetation modelling. For a region with a low density of gauges in Iran, Fallah et al. (2020) showed that ERA5 precipitation is closer to local observations than ERA-Interim but that GPCCv2018 (used here in bias correction or ERA5) is substantially better.
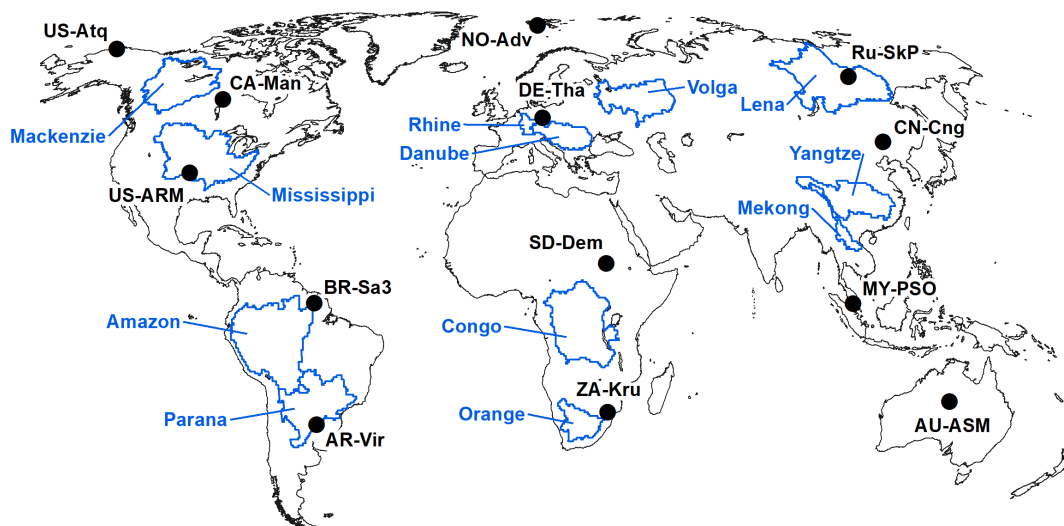
Figure 1. Location of FLUXNET2015 sites used to evaluate ERA5, WFDE5 and WFDEI as well as river basin outlines for the hydrological assessment.

4.2 Comparison with FLUXNET2015 and WFDEI

The FLUXNET2015 (FN2015) meteorological data (Chu, 2015; Pastorello et al., 2017) are not included in the data assimilation of the ERA5 reanalysis. Therefore, these data provide an opportunity to assess the degree to which the ERA5 and WFDE5 meteorological variables agree with surface observations. Despite there being over two hundred FN2015 sites globally they are highly clustered within Europe and North America. In order to provide a fairly uniform global assessment, 13 sites with at least three years of data have been selected from 12 countries spanning a wide range of longitudes and latitudes (Fig. 1, Table 4). The primary purpose of the FN2015 meteorological dataset is to provide data for forcing LSMs to allow comparison with the FN2015 surface exchange fluxes of energy and carbon. As such the FN2015 meteorological variables have been gap filled using ERA-Interim data to allow modelling without missing data. To avoid biasing the comparisons made here, only meteorological values that are measurements have been used (i.e. at times and locations where the FN2015 tier 1 quality flag is 0). Unfortunately, this means that some FN2015 sites do not provide observations for some variables at any time step ("Missing variables" in Table 4).

Two pairs of comparisons have been made: firstly for ERA5 (aggregated to half degree) versus FN2015 as well as for WFDE5 versus FN2015 at an hourly time step. This required converting the half-hourly FN2015 data to hourly steps and aligning the time stamps since ERA5 is on UTC instead of local time. ERA5 does not provide specific humidity so Qair was calculated using the 2 m air temperature, surface pressure and relative humidity using equations 4 and 6 of Buck (1981). The second comparisons were for WFDEI versus FN2015 as well as for WFDE5 versus FN2015 at 3-hourly time steps, again with alignment of time stamps. At each site mean bias error (MBE), mean absolute error (MAE) and correlation were calculated.

Table 4. Selected FLUXNET2015 sites.

Site code	Country	Site name	Longitude	Latitude	Start year	End year	Missing variables	DOI
US-Atq	USA	Atqauk	157.41ºW	70.47ºN	2006	2008	LWdown	10.18140/FLX/1440067
CA-Man	Canada	Manitoba	98.48ºW	55.88ºN	2006	2008	PSurf, LWdown	10.18140/FLX/1440035
US-ARM	USA	ARM Southern Great Plain site - Lamont	97.49ºW	36.61ºN	2010	2012		10.18140/FLX/1440066
BR-Sa3	Brazil	Santarem km67 primary forest	54.97ºW	3.02ºN	2001	2003		10.18140/FLX/1440033
AR-Vir	Argentina	Virasoro	56.19ºW	28.24ºS	2010	2012	LWdown, Precip	10.18140/FLX/1440192
NO-Adv*	Norway	Adventdalen	15.92ºE	78.19ºN	2012	2014		10.18140/FLX/1440241
DE-Tha	Germany	Tharandt	13.57ºE	50.96ºN	2012	2014		10.18140/FLX/1440152
SD-Dem	Sudan	Demokeya	30.48ºE	13.28ºN	2007	2009	LWdown	10.18140/FLX/1440186
ZA-Kru	South Africa	Skukuza	31.50ºE	25.02ºS	2008	2010	PSurf, LWdown	10.18140/FLX/1440188
RU-SkP	Russia	Yakutsk Spasskaya Pad larch	129.17ºE	62.26ºN	2010	2014	Precip	10.18140/FLX/1440243
CN-Cng	China	Chanling	123.51ºE	44.59ºN	2008	2010		10.18140/FLX/1440209
MY-PSO	Malaysia	Pasoh Forest Reserve	102.31ºE	2.97ºN	2007	2009	PSurf	10.18140/FLX/1440240
AU-ASM	Australia	Alice Springs	133.25ºE	22.28ºS	2011	2013		10.18140/FLX/1440194

*NO-Adv is now designated as SL-Adv (i.e. within Svalbard). Precip = precipitation. Note that "Missing variables" refers to tier 1 items provided by FLUXNET2015 as entirely gap-filled, not measured, values.

235 MAE was used instead of root mean square error since the former provides a less ambiguous basis for assessment (Willmott and Matsuura, 2005). Since the data are time series there is considerable serial correlation leading to spuriously high values. Consequently, the correlations of the previously pre-whitened time series – i.e. adjusted to remove lag-1 autocorrelation - are also reported as "adjusted correlation" (Ebisuzaki, 1997). Data for individual sites are reported for ERA5 and WFDE5 v FN2015 (hourly) in Tables A1 to A8 and for WFDEI and WFDE5 v FN2015 (3 hourly) in Tables A9 to A16. Average metrics

240 for the pairs of comparisons are shown in Fig. 2 and Tables A17 and A18.

At hourly steps on average there are no significant differences in MBE, MAE, correlation or adjusted correlation between ERA5 v FN2015 and WFDE5 v FN2015, for all variables apart from two (Fig. 2a). For air temperature the MBE is slightly better (closer to zero) for WFDE5 whereas the MAE is slightly worse (larger) for WFDE5. On the other hand, for specific humidity both the MBE and MAE are slightly worse for WFDE5. These results indicate that the bias and elevation corrections

245 incorporated into the WFDE5 have had little overall effect on the performance against surface observations compared to ERA5.

At three hourly steps, for all variables apart from precipitation, the average MBE plus 95% confidence intervals overlap zero for WFDEI and WFDE5 (Fig. 2b). For wind speed, downwards longwave and downwards shortwave the MAE is slightly better (smaller) for WFDE5 than WFDEI. For all variables, aside from precipitation, the MAE, correlation and adjusted correlation are slightly better for WFDE5 than WFDEI. For precipitation the MBE is slightly better and the correlation slightly higher for

250 WFDE5 versus WFDEI when corrected using the GPCC-, rather than CRU-precipitation totals. These results indicate that on average, at the FN2015 sites selected, WFDE5 performs better than WFDEI against the observations. Note that the average results in Fig. 2b and Table A17 hide the fact that for all metrics WFDEI data provide better results (MBE closer to 0.0, MAE lower, correlation higher) for some individual sites than WFDE5 (Tables A9 to A16). On the other hand, for Wind (speed) and Precipitation (CRU and GPCC corrected) the correlation and adjusted correlation are better for WFDE5 than WFDEI at every

255 site.
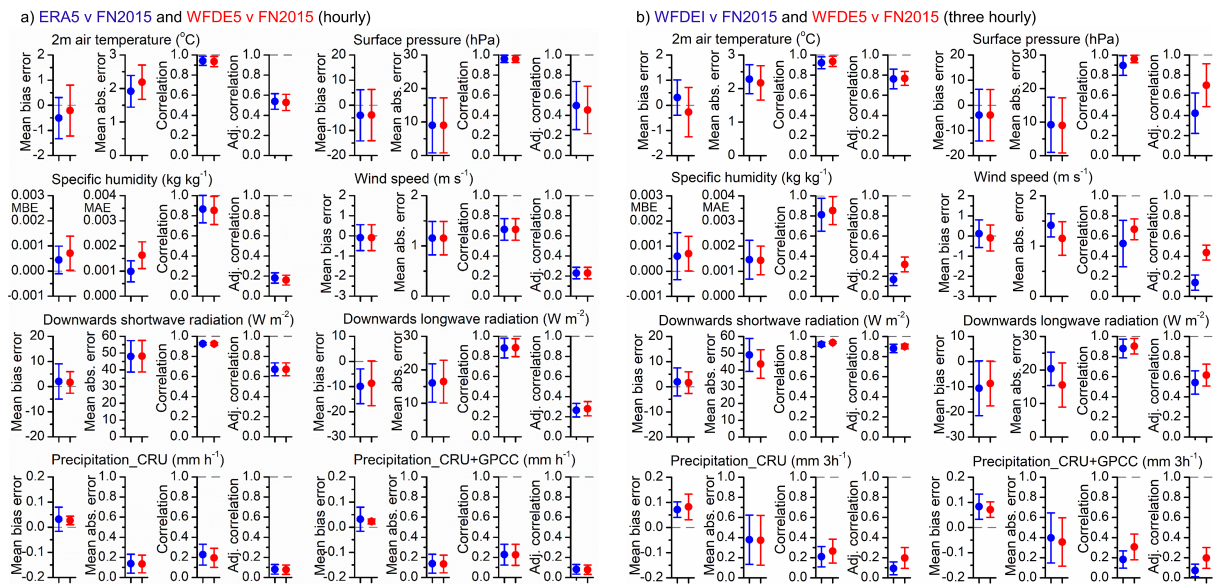
Figure 2. Average metrics (mean +/- 95% confidence interval of the mean) for: a) ERA5 v FN2015 (blue) and WFDE5 v FN2015 (red) at hourly time steps (see Table A17); b) WFDEI v FN2015 (blue) and WFDE5 v FN2015 (red) at three-hourly time steps (see Table A18).
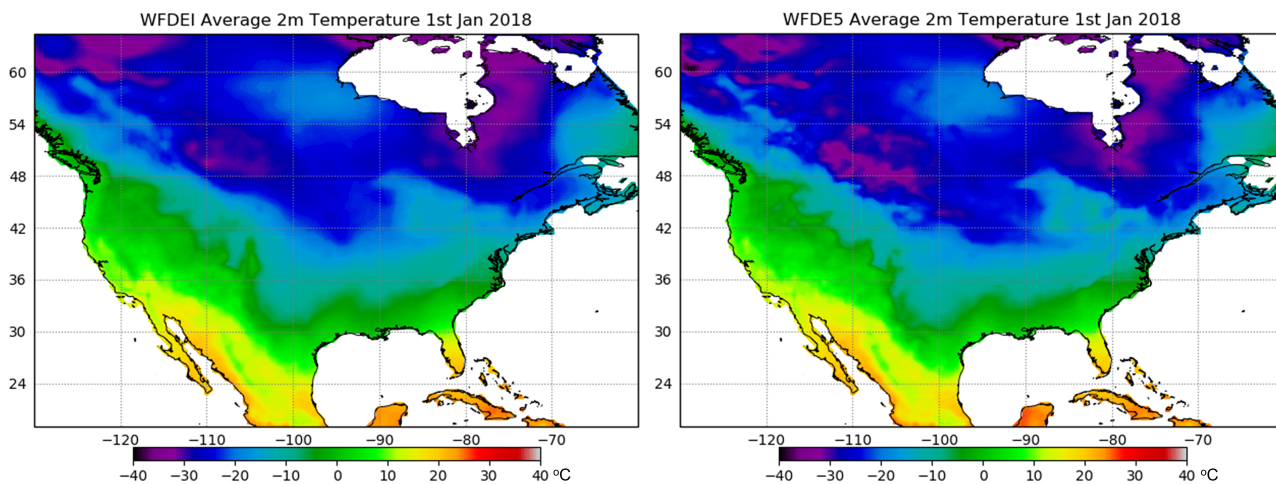
Figure 3. Average 2 m temperature on 1st January 2018 for north and central America.

Both WFDEI and WFDE5 in 2017 and 2018 are corrected using CRU TS4.03 so at monthly and longer scales there will be only small differences. However, at sub-monthly time scales, aside from advances in the processing system between the reanalyses used, it is likely that the better performance of WFDE5 is linked to superior spatial variability of ERA5 (data aggregated for WFDE5) versus ERA-Interim (data interpolated for WFDEI). This can be seen in the higher-resolution features of daily average temperature for a single day in January 2018 in north and central America in the WFDE5 data (Fig. 3).

Table 5. Long-term-annual water balance components [km^{3}yr^{-1}] as simulated with uncalibrated WaterGAP 2.2c for 1981-2010 and for global land area (except Antarctica and Greenland).

No	Component	ERA5	WFDE5_CRU+GPCC	WFDE5_CRU	WFDEI_CRU+GPCC	WFDEI_CRU
1	Precipitation	120245	111529	110981	111616	111554
2	Actual evapotranspiration	76695	73430	74702	73540	74230
3	River discharge to oceans and inland sinks	43623	38135	36310	38088	37320
4	Total (actual) water consumpitons (rows 5+6)	1105	1183	1151	1103	1086
5	Net (actual) abstraction from surface water	1241	1359	1318	1246	1223
6	Net abstraction from groundwater	-136	-176	-167	-143	-137
7	Change of total water storage	-74	-36	-31	-12	4
8	long-term annual water balance error	0.16	0.15	0.14	0.14	0.14

4.3 Validation with a global hydrological model

Of great importance for driving impact models such as global hydrological models is the climate forcing input since the water balance components are highly dependent on it (Müller Schmied et al., 2016). In order to test WFDE5 in terms of suitability for use with an impact model, the global water-availability and water-use model WaterGAP (version 2.2c, Müller Schmied et al., 2016) was used. WaterGAP calculates water storages and fluxes on global land area (except Antarctica) on a 0.5° × 0.5° resolution (55 × 55 km at the equator) and incorporates human interventions such as human water use and man-made reservoirs. Forcing requirements are daily values for precipitation (sum of rainfall and snowfall), average temperature, downwards shortwave radiation and downwards longwave radiation. For model specific details, the reader is referred to Müller Schmied et al. (2016, 2014) and Döll et al. (2003). Despite the possibility of calibrating the model, WaterGAP was run with an uncalibrated setup (model parameter γ set to 2, whereas CFA and CFS are set to 1 globally, details can be found in Müller Schmied et al. (2014)). This parameter choice was designated to mimic the behaviour in a typical impact model and also due to time and technical constraints (a time series start year of 1920 or earlier is required for standard calibration). The model was driven by ERA5, WFDE5 and WFDEI (the latter two with both the precipitation separately scaled to GPCC and CRU monthly sums and the daily aggregation of WFDE5 (W5E5; Lange, 2019c), see Sect. 5) and was assessed in terms of resulting water balance components (Table 5), for model efficiency (Fig. 4) and for river discharge seasonality for selected large river basins (Fig. 5).

The long-term-annual water balance shows considerably (around 10%) higher precipitation (P) for ERA5 compared to the WFDE5 adjustments to GPCC or CRU which results in higher values for actual evapotranspiration (AET) and greater river discharge to oceans and inland sinks (Q) (Table 5). The general reduction of mean global precipitation from 120000 km^{3}yr^{-1} for ERA5 to observation-based datasets with around 111000 km^{3}yr^{-1} for WFDE5 is consistent to previous estimates (109631 to 111050 km^{3}yr^{-1} for the time span 1971-2000 for the snow undercatch corrected climate forcings in Table 3 and 4 of Müller Schmied et al., 2016). Even though WaterGAP was not calibrated, AET and Q are well within the estimates of other models or
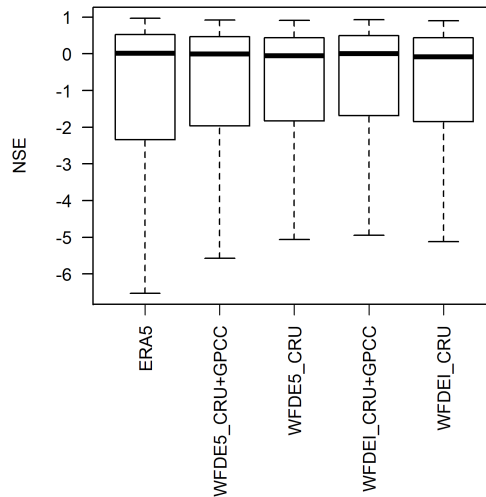
Figure 4. Model efficiency for the uncalibrated runs of the climate forcings in this assessment using monthly time series of 1216 GRDC stations.

datasets (AET 62800-75981 km^3yr^{-1} and Q 34400-44560 for most assessments according to Müller Schmied et al., 2014, Table 5). The differences in GPCC and CRU dataset versions to adjust ERA5 (ERA-Interim) precipitation for WFDE5 (WFDEI) is substantially smaller for GPCC (precipitation difference: 87 km^3yr^{-1} for WFDE5_CRU+GPCC vs. WFDEI_CRU+GPCC) compared to CRU (precipitation difference: 573 km^3yr^{-1} for WFDE5_CRU vs. WFDEI_CRU). Consequently, differences in simulated river discharge are higher for WFDE5_CRU vs. WFDEI_CRU (1010 km^3yr^{-1}) compared to WFDE5_CRU+GPCC vs. WFDEI_CRU+GPCC (47 km^3yr^{-1}). This implies that the choice of precipitation bias adjustment target (CRU or GPCC) impacts water balance components.

The performance of the uncalibrated model runs have been assessed using the widely used Nash Sutcliffe Efficiency metric (NSE, Nash and Sutcliffe, 1970) relative to monthly time series of GRDC station observed discharge. 1216 stations have been used out of the usual 1319 stations used for WaterGAP calibration (Müller Schmied et al., 2014) constrained by data availability for at least one year in the time span of the forcing. The optimum NSE is 1 and the value can become infinitely negative, but below 0 the simulation is not better than the average of the observations (Nash and Sutcliffe, 1970). The median performances of the model runs are similar and around the value 0 with some ranging towards optimum but also towards negative NSE values. Note that consistently around 16 to 17 % of the stations are outside of the limits of the boxplots (NSE > 1.5 * inter quartile range) towards negative values and not displayed. Generally, the variants scaled to GPCC tend to have a slightly better performance than the values scaled to CRU. Typically, the performance increases as a result of calibrating the model (see Müller Schmied et al., 2014, Fig. 6), so the NSE values reported here should not be wrongly interpreted as the result of a poor quality of forcing data but more towards that uncalibrated impact models could reach - in principle - similar efficiencies
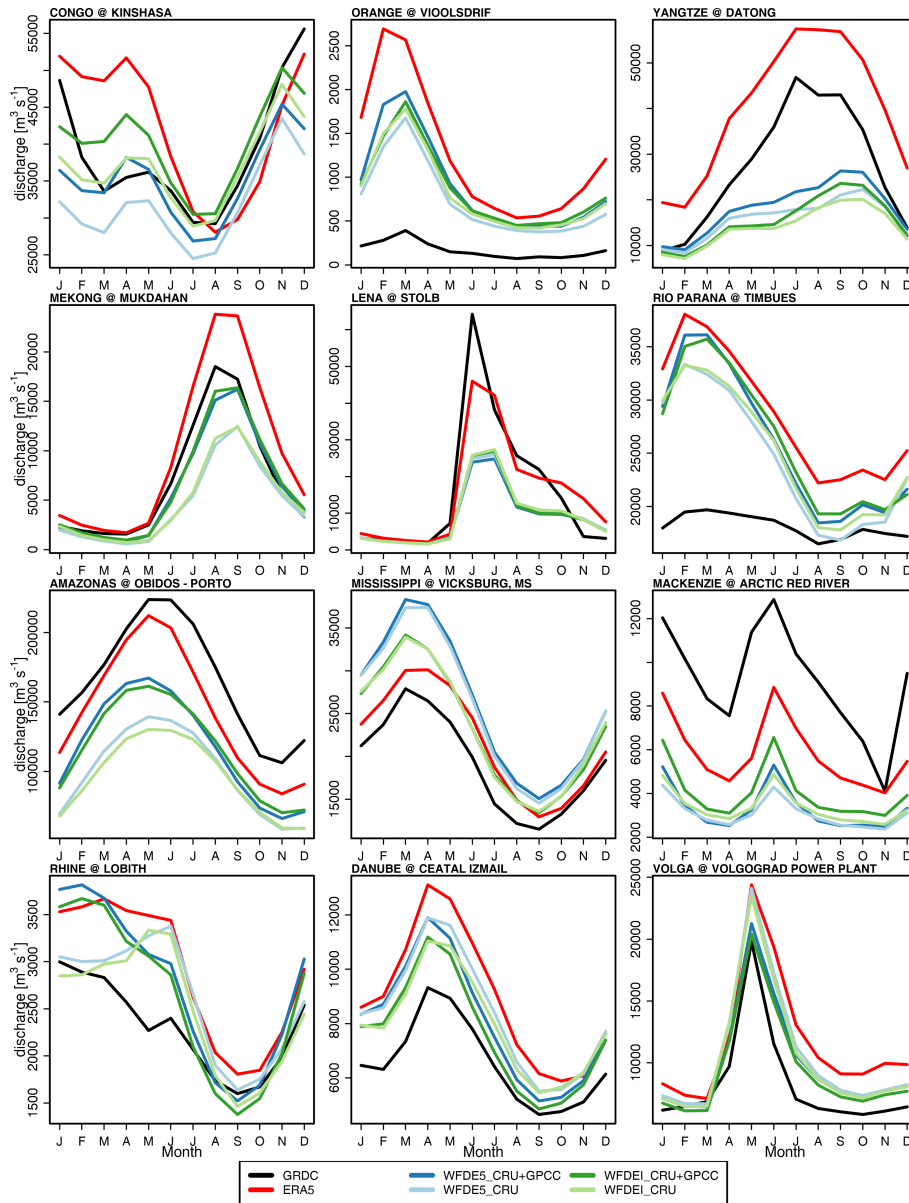
Figure 5. Seasonality of observed river discharge and uncalibrated WaterGAP runs for selected large river basins (Fig. 1).

independently of the forcing data assessed here (with slight advantages of the bias-adjusted WFDE5 data compared to direct use of ERA5, Fig. 4).

In Fig. 5 discharge seasonality is shown with GRDC observations in black – see Fig. 1 for basin outlines. The figure shows the effect of adjusting precipitation from ERA5 (red in Fig. 5). For most basins, but not for all (e.g. Mississippi), the adjustment

305   to CRU- or GPCC-precipitation leads to a reduction of river discharge - this is substantial for some basins, e.g. Yangtze and
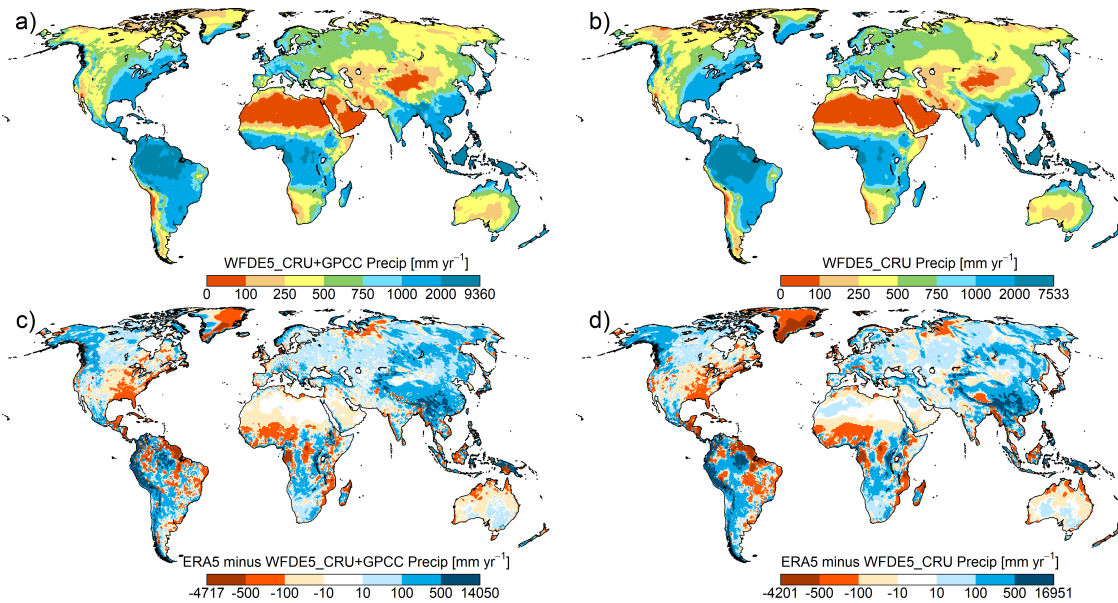
Figure 6. Long-term (1979–2016) average precipitation of the climate forcings, displayed as absolute number for WFDE5_CRU+GPCC (a), WFDE5_CRU (b) and differences to ERA5, computed as ERA5 minus WFDE5_CRU+GPCC (c) and ERA5 minus WFDE5_CRU (d). All units in $\mathrm{mm\ yr^{-1}}$.

Amazon. This does not necessarily lead to a better agreement with the observations (e.g. Amazon, Mackenzie, Lena), but for a number of basins it does (e.g. Congo, Orange, Mekong, Danube). Interestingly, the effect of the dataset chosen to adjust precipitation (CRU v GPCC) is important for some basins (e.g. Mekong, Amazon). However, this is not relevant for other basins (e.g. Mississippi, Danube) where differences in WFDE5 and WFDEI compared to ERA5 and ERA-Interim for variables other
310 than precipitation lead to different discharge simulations. An overview of spatial differences in long-term average precipitation between WFDE5 and ERA5 and can be found in Fig. 6 and help to interpret the patterns observed in Fig. 5. Spatial differences of the other variables used for WaterGAP are shown in Figs. A1 to A3.

The validation with WaterGAP showed that using WFDE5 generally results in similar results to using WFDEI and should be preferred to using ERA5 directly. Nevertheless, this assessment was done using uncalibrated runs, thus a proper calibration
315 to discharge observations could highlight the full benefit of WFDE5 compared to ERA5 but this is outside of the scope of this paper.

5 Application in ISIMIP

The WFDE5 dataset will be employed to drive historical impact simulations and bias-adjust future climate projections in the upcoming ISIMIP phase 3. The dataset is well suited for these purposes in particular thanks to its inter-variable consistency,
320 which matters for the simulation of extreme climate impact events (Zscheischler et al., 2019). Thanks to a new bias adjustment

method that is applied in ISIMIP phase 3, that is able to adjust inter-variable statistical dependencies (Lange, 2019b, 2020), the inter-variable consistency of WFDE5 will be beneficial for the bias adjustment of future climate projections as well.

Instead of using WFDE5 directly for these purposes, a derived dataset covering land and ocean with daily temporal resolution and including additional variables will be used in ISIMIP phase 3. This derived dataset consists of WFDE5 over land merged with ERA5 over the ocean (W5E5; Lange, 2019c). It covers land and ocean to facilitate impact studies everywhere and prevent mismatches between land-sea masks used by impact models. It has daily temporal resolution because that is sufficient to drive most impact models taking part in ISIMIP. Additional variables (2 m relative humidity, sea level pressure, total precipitation, daily maximum 2 m air temperature, daily minimum 2 m air temperature) derived from those included in WFDE5 are included in W5E5 to meet additional impact model requirements. More information about the W5E5 dataset is provided by Lange (2019c).

6 Conclusions

The WFDE5 dataset will be useful for forcing surface models especially for near-recent hydrological and agricultural analyses. It will also be used for bias correction of the CMIP6 GCM model output in the third phase of ISIMIP. WFDE5 benefits from the improvements of ERA5 compared to ERA-Interim as well as from the additional corrections of temperature, precipitation and shortwave radiation described above.

WFDE5 is provided at hourly time steps versus three-hourly for WFDEI. Comparison to observations from 13 FLUXNET2015 sites distributed globally shows that, on average, WFDE5 is superior to WFDEI for all variables in terms of mean absolute error and correlation. For precipitation and wind speed WFDE5 is superior to WFDEI at all 13 sites. Although both datasets are provided at 0.5° resolution, WFDE5 has a greater spatial variability (Fig. 3) since it is obtained by aggregation of higher resolution ERA5 data rather than by interpolation of lower resolution ERA-Interim data used in WFDEI. Initial analysis using an uncalibrated hydrological model (WaterGAP) has demonstrated that the bias correction to CRU or GPCC precipitation totals results in lower discharge throughout the year bringing the global hydrological balance into better agreement with previous studies. The corrections result in improvements towards observations relative to the use of unaltered ERA5 forcing (e.g. in the Congo, Orange and Danube basins).

Currently the WFDE5 datasets spans from the start of 1979 to the end of 2018 (end of 2016 for Rainf_WFDE5_CRU+GPCC and Snowf_WFDE5_CRU+GPCC). However, the open source Python code within the Climate Change Service Toolbox will allow users to expand the coverage back to the start of 1950 and forwards through 2019 and later for themselves. The data have been created at 0.5° resolution to match the CRU grid, but gridded observations of precipitation totals are already available from GPCC at 0.25° and MSWEPv2 at 0.1° (Beck et al., 2019b). The future availability of gridded observations of near-surface temperature, diurnal temperature range, cloud cover, aerosol loading and numbers of wet days would allow creation of WFDE5 data at higher spatial resolution than the current dataset.

Appendix A

Table A1. Tair metrics for each FLUXNET2015 site: ERA5 v FN2015 and WFDE5 v FN2015, hourly time steps.

Tair (°C)	No. points	Mean Fluxnet 2015	MBE		MAE		Correlation		Adj. Correlation	
			ERA5	WFDE5	ERA5	WFDE5	ERA5	WFDE5	ERA5	WFDE5
US-Atq	26227	-10.127	0.529	0.514	2.035	2.712	0.984	0.977	0.451	0.401
CA-Man	20062	0.741	-1.620	-2.138	1.949	2.452	0.992	0.988	0.727	0.712
US-ARM	23442	15.451	0.856	1.999	1.703	1.999	0.978	0.977	0.745	0.744
BR-Sa3	24500	25.874	0.449	1.125	1.668	2.044	0.724	0.689	0.381	0.383
AR-Vir	18209	21.750	-0.199	0.034	1.501	1.541	0.958	0.958	0.574	0.572
NO-Adv	12039	-2.298	-1.797	-1.657	2.080	2.093	0.980	0.969	0.469	0.409
DE-Tha	26298	9.324	-1.060	-0.023	1.588	1.714	0.973	0.968	0.634	0.629
SD-Dem	24624	27.058	0.072	1.217	1.386	1.858	0.956	0.952	0.638	0.640
ZA-Kru	24825	21.701	-1.424	-0.631	2.194	2.446	0.887	0.878	0.425	0.427
RU-SkP	22123	-2.740	-3.891	-4.262	4.276	4.650	0.984	0.982	0.331	0.330
CN-Cng	24117	6.760	0.321	0.303	1.320	1.354	0.994	0.994	0.526	0.520
MY-PSO	26295	25.066	0.753	1.153	1.155	1.401	0.884	0.879	0.593	0.594
AU-ASM	26239	22.695	-0.269	-0.353	2.082	2.200	0.950	0.946	0.502	0.501

Table A2. PSurf metrics for each FLUXNET2015 site: ERA5 v FN2015 and WFDE5 v FN2015, hourly time steps.

PSurf (hPa)	No. points	Mean	MBE		MAE		Correlation		Adj. Correlation	
		Fluxnet 2015	ERA5	WFDE5	ERA5	WFDE5	ERA5	WFDE5	ERA5	WFDE5
US-Atq	17345	1012.4	-2.8	-2.8	2.8	2.8	0.986	0.986	0.050	0.050
US-ARM	24196	976.3	0.4	0.5	0.6	0.6	0.997	0.996	0.733	0.656
BR-Sa3	22274	986.1	15.0	15.0	15.0	15.0	0.880	0.880	0.051	0.060
AR-Vir	18048	999.2	4.1	4.1	4.1	4.1	0.992	0.992	0.883	0.797
NO-Adv	12038	1011.3	-39.5	-39.4	39.5	39.4	0.994	0.994	0.847	0.845
DE-Tha	26301	972.3	-9.1	-8.9	9.1	8.9	0.997	0.997	0.378	0.166
SD-Dem	6636	949.6	-8.4	-8.2	8.5	8.2	0.978	0.972	0.551	0.695
RU-SkP	22128	987.5	-2.3	-2.4	2.3	2.4	0.996	0.996	0.913	0.726
CN-Cng	24117	992.0	5.0	4.9	5.6	5.6	0.867	0.867	0.312	0.085
AU-ASM	26200	945.0	-2.1	-2.2	2.9	2.9	0.930	0.930	0.254	0.453

Table A3. Qair metrics for each FLUXNET2015 site: ERA5 v FN2015 and WFDE5 v FN2015, hourly time steps.

Qair $(kg\ kg^{-1})$	No. points	Mean	MBE		MAE		Correlation		Adj. Correlation	
		Fluxnet 2015	ERA5	WFDE5	ERA5	WFDE5	ERA5	WFDE5	ERA5	WFDE5
US-Atq	26304	0.00242	-0.00010	-0.00031	0.00031	0.00046	0.963	0.946	0.257	0.169
CA-Man	26235	0.00410	-0.00049	-0.00063	0.00088	0.00095	0.928	0.925	0.135	0.158
US-ARM	26294	0.00771	0.00026	0.00053	0.00095	0.00106	0.955	0.949	0.174	0.172
BR-Sa3	26280	0.01537	0.00288	0.00365	0.00295	0.00370	0.208	0.201	-0.020	-0.033
AR-Vir	26299	0.01123	0.00056	0.00074	0.00130	0.00142	0.866	0.859	0.120	0.126
NO-Adv	26234	0.00271	-0.00033	-0.00035	0.00039	0.00043	0.979	0.964	0.228	0.199
DE-Tha	26304	0.00573	-0.00030	0.00077	0.00049	0.00086	0.975	0.969	0.291	0.268
SD-Dem	26304	0.00800	0.00042	0.00089	0.00106	0.00134	0.963	0.959	0.205	0.192
ZA-Kru	26304	0.01072	0.00016	0.00079	0.00095	0.00142	0.922	0.894	0.169	0.074
RU-SkP	21505	0.00358	0.00007	0.00004	0.00054	0.00058	0.970	0.966	0.128	0.110
CN-Cng	26303	0.00486	0.00023	0.00021	0.00052	0.00051	0.988	0.987	0.312	0.301
MY-PSO	26304	0.01634	0.00157	0.00201	0.00160	0.00203	0.577	0.520	0.132	0.133
AU-ASM	26304	0.00606	0.00082	0.00083	0.00098	0.00103	0.962	0.853	0.218	0.207

Table A4. Wind metrics for each FLUXNET2015 site: ERA5 v FN2015 and WFDE5 v FN2015, hourly time steps.

Wind (m s^{-1})	No. points	Mean Fluxnet 2015	MBE		MAE		Correlation		Adj. Correlation	
			ERA5	WFDE5	ERA5	WFDE5	ERA5	WFDE5	ERA5	WFDE5
US-Atq	19078	3.587	1.233	1.233	1.454	1.454	0.840	0.840	0.251	0.251
CA-Man	17111	3.403	-0.251	-0.251	0.684	0.684	0.790	0.790	0.254	0.254
US-ARM	21285	4.636	-0.320	-0.320	1.103	1.103	0.816	0.816	0.308	0.308
BR-Sa3	23365	2.229	-0.542	-0.542	0.835	0.835	0.296	0.296	0.113	0.113
AR-Vir	18002	2.317	0.821	0.821	0.998	0.998	0.677	0.677	0.217	0.217
NO-Adv	6778	5.394	-2.690	-2.690	2.744	2.744	0.714	0.714	0.354	0.354
DE-Tha	25974	3.033	-0.157	-0.157	0.899	0.899	0.672	0.672	0.154	0.154
SD-Dem	24620	2.848	0.897	0.897	1.274	1.273	0.583	0.583	0.271	0.271
ZA-Kru	24825	3.242	-1.160	-1.160	1.309	1.309	0.645	0.645	0.241	0.241
RU-SkP	16790	2.748	-0.042	-0.042	0.616	0.616	0.786	0.786	0.182	0.182
CN-Cng	24096	3.670	0.080	0.080	0.904	0.904	0.821	0.821	0.305	0.305
MY-PSO	26061	1.785	-0.303	-0.303	0.769	0.769	0.317	0.317	0.019	0.019
AU-ASM	26213	2.565	1.289	1.289	1.430	1.430	0.675	0.675	0.322	0.322

Table A5. SWdown metrics for each FLUXNET2015 site: ERA5 v FN2015 and WFDE5 v FN2015, hourly time steps.

SWdown (W m^{-2})	No. points	Mean Fluxnet 2015	MBE		MAE		Correlation		Adj. Correlation	
			ERA5	WFDE5	ERA5	WFDE5	ERA5	WFDE5	ERA5	WFDE5
US-Atq	25819	106.825	-16.268	-16.318	31.256	31.304	0.932	0.932	0.679	0.679
CA-Man	22867	132.639	0.883	0.698	42.677	42.601	0.916	0.916	0.612	0.612
US-ARM	24056	195.043	1.182	2.389	46.446	46.531	0.951	0.951	0.785	0.784
BR-Sa3	24000	186.600	8.492	8.470	65.037	65.200	0.892	0.892	0.568	0.568
AR-Vir	15829	93.032	3.217	3.742	33.260	33.490	0.925	0.924	0.654	0.654
NO-Adv	12174	87.650	4.177	4.280	28.848	28.880	0.901	0.900	0.477	0.477
DE-Tha	26164	124.441	1.696	3.955	39.427	39.607	0.927	0.927	0.601	0.601
SD-Dem	24386	257.052	12.876	12.149	50.778	50.612	0.965	0.965	0.878	0.878
ZA-Kru	20650	196.204	2.050	1.279	53.103	52.882	0.932	0.932	0.715	0.715
RU-SkP	21726	128.763	1.521	0.161	45.401	45.304	0.916	0.916	0.631	0.631
CN-Cng	25305	163.944	9.518	8.084	41.196	41.016	0.949	0.949	0.765	0.765
MY-PSO	26084	193.032	0.169	-5.169	62.153	62.170	0.910	0.909	0.614	0.613
AU-ASM	26210	255.772	-3.263	-2.342	84.963	86.203	0.918	0.917	0.740	0.740

Table A6. LWdown metrics for each FLUXNET2015 site: ERA5 v FN2015 and WFDE5 v FN2015, hourly time steps.

LWdown (W m^{-2})	No. points	Mean Fluxnet 2015	MBE ERA5	MBE WFDE5	MAE ERA5	MAE WFDE5	Correlation ERA5	Correlation WFDE5	Adj. Correlation ERA5	Adj. Correlation WFDE5
US-ARM	24106	335.275	-5.157	-1.555	13.372	13.281	0.964	0.962	0.342	0.366
BR-Sa3	18705	417.810	-3.479	2.234	10.979	10.591	0.699	0.729	0.303	0.336
NO-Adv	11092	287.082	-26.027	-28.481	30.119	32.124	0.880	0.868	0.153	0.159
DE-Tha	26301	315.195	-7.511	-2.397	15.473	14.744	0.901	0.898	0.208	0.216
RU-SkP	21963	261.041	-17.763	-20.020	22.163	23.999	0.972	0.970	0.169	0.182
CN-Cng	21700	287.760	-11.902	-11.579	14.911	14.822	0.980	0.980	0.318	0.325
MY-PSO	26263	417.346	-2.314	-1.719	11.217	10.728	0.700	0.722	0.256	0.277
AU-ASM	26221	346.663	-5.025	-6.203	10.320	11.483	0.969	0.964	0.372	0.377

Table A7. Precipitation (Rainf + Snowf) metrics, corrected using CRU totals, for each FLUXNET2015 site: ERA5 v FN2015 and WFDE5 v FN2015, hourly time steps.

P. CRU (mm h^{-1})	No. points	Mean Fluxnet 2015	MBE ERA5	MBE WFDE5	MAE ERA5	MAE WFDE5	Correlation ERA5	Correlation WFDE5	Adj. Correlation ERA5	Adj. Correlation WFDE5
US-Atq	26133	0.104	0.018	0.014	0.035	0.032	0.135	0.066	0.046	0.022
CA-Man	13634	0.042	0.047	0.029	0.097	0.085	0.232	0.195	0.079	0.074
US-ARM	24114	0.056	0.024	0.045	0.098	0.114	0.292	0.272	0.112	0.102
Br-Sa3	26280	0.161	0.089	0.078	0.374	0.366	0.044	0.038	0.014	0.013
NO-Adv	6516	0.018	0.048	0.052	0.064	0.071	0.366	0.239	0.097	0.060
DE-Tha	26304	0.097	0.000	-0.013	0.113	0.104	0.412	0.412	0.180	0.173
SD-Dem	24621	0.032	-0.008	0.008	0.053	0.068	0.061	0.060	0.006	0.002
ZA-Kru	24818	0.044	0.043	0.033	0.110	0.101	0.179	0.174	0.045	0.038
CN-Cng	24117	0.037	0.023	0.017	0.062	0.059	0.516	0.455	0.233	0.194
MY-PSO	26301	0.220	0.068	0.029	0.455	0.420	0.079	0.075	0.017	0.014
AU-ASM	26234	0.032	0.002	0.001	0.051	0.055	0.182	0.159	0.064	0.072

Table A8. Precipitation (Rainf + Snowf) metrics, corrected using GPCC totals, for each FLUXNET2015 site: ERA5 v FN2015 and WFDE5 v FN2015, hourly time steps.

P. GPCC (mm h^{-1})	No. points	Mean Fluxnet 2015	MBE		MAE		Correlation		Adj. Correlation	
			ERA5	WFDE5	ERA5	WFDE5	ERA5	WFDE5	ERA5	WFDE5
US-Atq	26133	0.104	0.018	0.006	0.035	0.024	0.135	0.098	0.046	0.025
CA-Man	13634	0.042	0.047	0.042	0.097	0.094	0.232	0.220	0.079	0.079
US-ARM	24114	0.056	0.024	0.027	0.098	0.099	0.292	0.312	0.112	0.115
BR-Sa3	26280	0.161	0.089	0.045	0.374	0.333	0.044	0.055	0.014	0.019
NO-Adv	6516	0.018	0.048	0.028	0.064	0.049	0.366	0.332	0.097	0.079
DE-Tha	26304	0.097	0.000	0.016	0.113	0.116	0.412	0.424	0.180	0.174
SD-Dem	24621	0.032	-0.008	0.015	0.053	0.074	0.061	0.062	0.006	0.002
ZA-Kru	24818	0.044	0.043	0.036	0.110	0.102	0.179	0.189	0.045	0.042
CN-Cng	24117	0.037	0.023	0.008	0.062	0.050	0.516	0.522	0.233	0.213
MY-PSO	26301	0.220	0.068	0.034	0.455	0.423	0.079	0.079	0.017	0.016
AU-ASM	26234	0.032	0.002	0.001	0.051	0.050	0.182	0.185	0.064	0.083

Table A9. Tair metrics for each FLUXNET2015 site: WFDEI v FN2015 and WFDE5 v FN2015, 3-hourly time steps.

Tair (°C)	No. points	Mean	MBE		MAE		Correlation		Adj. Correlation	
		Fluxnet 2015	WFDEI	WFDE5	WFDEI	WFDE5	WFDEI	WFDE5	WFDEI	WFDE5
US-Atq	8736	-10.124	1.210	0.528	2.991	2.729	0.975	0.977	0.562	0.608
CA-Man	6687	0.741	-2.198	-2.086	2.729	2.453	0.984	0.987	0.827	0.830
US-ARM	7821	15.445	1.671	1.538	2.402	2.048	0.968	0.977	0.864	0.897
BR-Sa3	8162	25.866	1.278	1.149	2.167	2.039	0.701	0.687	0.715	0.689
AR-Vir	6071	21.759	0.207	0.058	1.619	1.542	0.950	0.959	0.848	0.869
NO-Adv	4016	-2.264	-1.148	-1.663	2.222	2.099	0.941	0.969	0.381	0.562
DE-Tha	8766	9.333	-0.042	-0.030	1.793	1.708	0.965	0.969	0.760	0.814
SD-Dem	8208	27.119	0.888	1.096	1.682	1.732	0.954	0.956	0.923	0.894
ZA-Kru	8274	21.722	-0.710	-0.634	2.266	2.578	0.909	0.874	0.832	0.704
RU-SkP	7373	-2.722	-3.572	-4.295	4.192	4.620	0.982	0.982	0.705	0.706
CN-Cng	8035	6.780	-0.027	0.184	1.977	1.573	0.986	0.991	0.778	0.687
MY-PSO	8761	25.062	1.372	1.121	2.055	1.385	0.711	0.881	0.662	0.819
AU-ASM	8743	22.763	-0.468	-0.459	1.534	1.686	0.971	0.969	0.905	0.901

Table A10. PSurf metrics for each FLUXNET2015 site: WFDEI v FN2015 and WFDE5 v FN2015, 3-hourly time steps.

PSurf (hPa)	No. points	Mean	MBE		MAE		Correlation		Adj. Correlation	
		Fluxnet 2015	WFDEI	WFDE5	WFDEI	WFDE5	WFDEI	WFDE5	WFDEI	WFDE5
US-Atq	5779	1012.4	-2.9	-2.8	3.0	2.8	0.976	0.986	0.465	0.283
US-ARM	8065	976.3	0.6	0.5	1.3	0.6	0.977	0.996	0.576	0.929
BR-Sa3	7451	986.1	15.3	15.0	15.3	15.0	0.576	0.879	0.421	0.981
AR-Vir	6022	999.1	4.0	4.1	4.0	4.1	0.966	0.992	0.265	0.720
NO-Adv	4015	1011.3	-39.6	-39.4	39.7	39.4	0.983	0.994	0.922	0.983
DE-Tha	8766	972.3	-8.8	-8.9	8.8	8.9	0.983	0.997	0.269	0.955
SD-Dem	2210	949.6	-8.4	-8.2	8.4	8.2	0.744	0.974	0.064	0.466
RU-SkP	7375	987.5	-2.4	-2.4	2.4	2.4	0.993	0.996	0.813	0.886
CN-Cng	8035	992.0	5.2	5.0	5.9	5.6	0.867	0.865	0.284	0.203
AU-ASM	8732	945.0	-2.1	-2.2	2.9	2.9	0.892	0.929	0.130	0.590

Table A11. Qair metrics for each FLUXNET2015 site: WFDEI v FN2015 and WFDE5 v FN2015, 3-hourly time steps.

Qair (kg kg^{-1})	No. points	Mean Fluxnet 2015	MBE		MAE		Correlation		Adj. Correlation	
			WFDEI	WFDE5	WFDEI	WFDE5	WFDEI	WFDE5	WFDEI	WFDE5
US-Atq	8764	0.00242	-0.00004	-0.00031	0.00040	0.00046	0.954	0.946	0.334	0.298
CA-Man	8741	0.00410	-0.00077	-0.00063	0.00106	0.00095	0.914	0.924	0.073	0.327
US-ARM	8763	0.00772	-0.00038	0.00048	0.00143	0.00105	0.903	0.949	0.184	0.364
BR-Sa3	8758	0.01538	0.00509	0.00370	0.00514	0.00375	0.113	0.215	0.018	0.070
AR-Vir	8765	0.01124	-0.00007	0.00069	0.00166	0.00140	0.811	0.862	0.126	0.297
NO-Adv	8742	0.00271	-0.00001	-0.00035	0.00038	0.00043	0.946	0.964	0.186	0.414
DE-Tha	8767	0.00573	0.00048	0.00077	0.00077	0.00086	0.941	0.969	0.107	0.444
SD-Dem	8767	0.00800	0.00077	0.00089	0.00139	0.00134	0.942	0.959	0.247	0.387
ZA-Kru	8767	0.01072	0.00106	0.00077	0.00189	0.00143	0.852	0.892	0.078	0.132
RU-SkP	7186	0.00359	-0.00008	0.00002	0.00061	0.00058	0.960	0.966	0.200	0.258
CN-Cng	8766	0.00486	-0.00041	0.00023	0.00071	0.00053	0.974	0.987	0.366	0.497
MY-PSO	8766	0.01633	0.00216	0.00205	0.00257	0.00206	0.320	0.506	0.159	0.215
AU-ASM	8765	0.00606	-0.00005	0.00084	0.00094	0.00102	0.921	0.956	0.090	0.437

Table A12. Wind metrics for each FLUXNET2015 site: WFDEI v FN2015 and WFDE5 v FN2015, 3-hourly time steps.

Wind (m s^{-1})	No. points	Mean Fluxnet 2015	MBE		MAE		Correlation		Adj. Correlation	
			WFDEI	WFDE5	WFDEI	WFDE5	WFDEI	WFDE5	WFDEI	WFDE5
US-Atq	6352	3.583	1.021	1.234	1.538	1.459	0.718	0.838	0.234	0.465
CA-Man	5683	3.404	-1.092	-0.251	1.270	0.687	0.644	0.792	0.184	0.504
US-ARM	7077	4.630	0.031	-0.306	1.351	1.091	0.709	0.820	0.232	0.582
BR-Sa3	7791	2.242	-0.829	-0.553	0.998	0.837	0.273	0.323	0.133	0.259
AR-Vir	5994	2.326	1.471	0.803	1.612	0.985	0.535	0.678	0.080	0.451
NO-Adv	2232	5.404	-1.217	-2.699	1.828	2.748	0.597	0.719	0.287	0.521
DE-Tha	8659	3.037	0.332	-0.155	1.090	0.901	0.613	0.671	0.074	0.336
SD-Dem	8206	2.870	1.403	0.892	1.839	1.264	0.339	0.581	0.007	0.440
ZA-Kru	8274	3.234	-1.580	-1.166	1.676	1.311	0.446	0.643	0.190	0.451
RU-SkP	5599	2.749	-0.732	-0.041	0.946	0.617	0.642	0.785	0.176	0.398
CN-Cng	8025	3.669	0.415	0.078	1.175	0.905	0.736	0.820	0.321	0.583
MY-PSO	8682	1.790	0.368	-0.321	0.951	0.763	0.129	0.328	-0.054	0.160
AU-ASM	8736	2.591	1.935	1.269	2.110	1.408	0.439	0.676	-0.080	0.501

Table A13. SWdown metrics for each FLUXNET2015 site: WFDEI v FN2015 and WFDE5 v FN2015, 3-hourly time steps.

SWdown (W m^{-2})	No. points	Mean Fluxnet 2015	MBE		MAE		Correlation		Adj. Correlation	
			WFDEI	WFDE5	WFDEI	WFDE5	WFDEI	WFDE5	WFDEI	WFDE5
US-Atq	8560	107.382	-19.644	-16.391	32.138	29.791	0.936	0.939	0.893	0.896
CA-Man	7458	132.364	2.851	0.400	41.355	38.663	0.926	0.930	0.883	0.891
US-ARM	7874	188.303	5.887	2.023	49.891	42.040	0.941	0.958	0.925	0.940
BR-Sa3	7691	188.557	-9.459	8.683	54.996	54.881	0.916	0.920	0.902	0.896
AR-Vir	4676	104.609	1.621	4.166	36.737	34.126	0.925	0.936	0.874	0.887
NO-Adv	3920	86.934	7.180	4.652	37.221	25.975	0.862	0.916	0.710	0.804
DE-Tha	8659	124.362	7.860	3.860	63.740	34.543	0.857	0.945	0.759	0.901
SD-Dem	7961	256.791	5.962	12.491	52.392	47.142	0.964	0.970	0.955	0.962
ZA-Kru	6726	198.571	18.201	1.109	59.145	47.306	0.929	0.946	0.912	0.927
RU-SkP	6983	130.778	-4.122	-0.976	26.017	41.382	0.961	0.930	0.934	0.871
CN-Cng	8380	164.232	6.550	8.133	36.527	37.803	0.953	0.958	0.934	0.936
MY-PSO	8606	189.032	0.059	-4.660	62.236	51.765	0.899	0.933	0.881	0.906
AU-ASM	8710	254.611	2.086	-2.195	85.343	81.440	0.919	0.927	0.887	0.893

Table A14. LWdown metrics for each FLUXNET2015 site: WFDEI v FN2015 and WFDE5 v FN2015, 3-hourly time steps.

LWdown (W m^{-2})	No. points	Mean Fluxnet 2015	MBE		MAE		Correlation		Adj. Correlation	
			WFDEI	WFDE5	WFDEI	WFDE5	WFDEI	WFDE5	WFDEI	WFDE5
US-ARM	8013	335.283	-7.250	-1.556	15.759	12.448	0.955	0.967	0.632	0.703
BR-Sa3	6103	417.552	16.713	2.293	19.635	9.403	0.738	0.762	0.707	0.727
NO-Adv	3581	287.692	-29.268	-28.467	33.945	31.531	0.872	0.881	0.258	0.366
DE-Tha	8765	315.184	-10.346	-2.396	17.538	13.257	0.897	0.916	0.442	0.568
RU-SkP	7280	260.923	-19.107	-20.013	23.150	23.341	0.971	0.973	0.527	0.491
CN-Cng	7189	288.124	-14.132	-11.582	17.637	14.097	0.977	0.983	0.558	0.663
MY-PSO	8728	417.274	-11.149	-1.690	18.903	9.322	0.684	0.768	0.621	0.681
AU-ASM	8727	346.601	-10.148	-6.204	16.340	10.773	0.946	0.970	0.591	0.729

Table A15. Precipitation (Rainf + Snowf) metrics, corrected using CRU totals, for each FLUXNET2015 site: WFDEI v FN2015 and WFDE5 v FN2015, 3-hourly time steps.

P. CRU (mm 3h^{-1})	No. points	Mean Fluxnet 2015	MBE		MAE		Correlation		Adj. Correlation	
			WFDEI	WFDE5	WFDEI	WFDE5	WFDEI	WFDE5	WFDEI	WFDE5
US-Atq	8700	0.031	0.027	0.043	0.081	0.095	0.075	0.082	0.029	0.051
CA-Man	4454	0.122	0.126	0.092	0.280	0.236	0.211	0.282	0.068	0.209
US-ARM	8016	0.166	0.078	0.137	0.299	0.312	0.271	0.368	0.141	0.253
Br-Sa3	8758	0.482	0.139	0.235	0.929	1.033	0.083	0.063	0.029	0.030
NO-Adv	2132	0.055	0.072	0.158	0.141	0.208	0.206	0.277	0.069	0.188
DE-Tha	8767	0.291	0.046	-0.039	0.353	0.265	0.467	0.552	0.220	0.387
SD-Dem	8203	0.097	0.039	0.025	0.218	0.196	0.042	0.092	0.026	0.043
ZA-Kru	8266	0.133	0.119	0.100	0.317	0.283	0.223	0.263	0.105	0.106
CN-Cng	8036	0.111	0.032	0.052	0.168	0.157	0.483	0.575	0.307	0.444
MY-PSO	8764	0.661	0.103	0.088	1.239	1.172	0.078	0.131	-0.012	0.055
AU-ASM	8739	0.095	-0.001	0.016	0.149	0.149	0.182	0.246	0.052	0.121

Table A16. Precipitation (Rainf + Snowf) metrics, corrected using GPCC totals, for each FLUXNET2015 site: WFDEI v FN2015 and WFDE5 v FN2015, 3-hourly time steps.

P. GPCC (mm 3h^{-1})	No. points	Mean Fluxnet 2015	MBE		MAE		Correlation		Adj. Correlation	
			WFDEI	WFDE5	WFDEI	WFDE5	WFDEI	WFDE5	WFDEI	WFDE5
US-Atq	8721	0.031	0.044	0.018	0.097	0.071	0.058	0.127	0.029	0.070
CA-Man	4454	0.121	0.101	0.131	0.264	0.259	0.200	0.312	0.070	0.225
US-ARM	8016	0.166	0.122	0.082	0.337	0.268	0.255	0.424	0.138	0.288
BR-Sa3	8758	0.482	0.247	0.135	1.028	0.936	0.071	0.088	0.026	0.048
NO-Adv	2132	0.055	0.131	0.085	0.195	0.142	0.148	0.385	0.051	0.268
DE-Tha	8767	0.291	-0.052	0.047	0.316	0.295	0.444	0.569	0.227	0.395
SD-Dem	8203	0.097	0.052	0.046	0.231	0.214	0.043	0.095	0.019	0.042
ZA-Kru	8266	0.133	0.097	0.107	0.302	0.287	0.192	0.292	0.085	0.099
CN-Cng	8038	0.111	0.063	0.023	0.201	0.133	0.348	0.654	0.214	0.508
MY-PSO	8764	0.661	0.087	0.101	1.229	1.180	0.072	0.139	-0.011	0.062
AU-ASM	8739	0.095	0.023	0.002	0.166	0.135	0.183	0.288	0.066	0.164

Table A17. Average metrics across all 13 FLUXNET2015 sites +/- 95% confidence intervals of the means for ERA5 v FN2015 and WFDE5 v FN2015 at hourly time steps (see Appendix tables A1 to A8).

Variable	No. sites	Ave. MBE		Ave. MAE		Ave. Correlation		Ave. Adj. Correlation	
		ERA5	WFDE5	ERA5	WFDE5	ERA5	WFDE5	ERA5	WFDE5
Tair (°C)	13	-0.560	-0.209	1.918	2.190	0.942	0.935	0.538	0.528
		±0.820	±1.015	±0.472	±0.512	±0.045	±0.050	±0.077	±0.080
PSurf (hPa)	10	-4.0	-3.9	9.0	9.0	0.962	0.961	0.497	0.453
		±10.2	±10.2	±8.2	±8.2	±0.036	±0.036	±0.240	±0.236
Qair (kg kg^{-1})	13	0.00044	0.00071	0.00099	0.00163	0.866	0.853	0.181	0.160
		±0.00055	±0.00068	±0.00042	±0.00053	±0.136	±0.140	±0.051	±0.049
Wind (m s^{-1})	13	-0.088	-0.088	1.155	1.155	0.664	0.664	0.230	0.230
		±0.646	±0.646	±0.333	±0.333	±0.107	±0.107	±0.057	±0.057
SWdown (W m^{-2})	13	2.019	1.644	48.042	48.138	0.926	0.925	0.671	0.671
		±7.013	±4.287	±9.415	±9.554	±0.012	±0.013	±0.064	±0.064
LWdown (W m^{-2})	8	-9.897	-8.715	16.069	16.473	0.883	0.887	0.265	0.280
		±6.900	±8.900	±5.706	±6.398	±0.099	±0.089	±0.068	±0.071
P. CRU (mm h^{-1})	11	0.032	0.027	0.137	0.134	0.227	0.195	0.081	0.069
		±0.048	±0.017	±0.094	±0.088	±0.103	±0.095	±0.048	±0.043
P. GPCC (mm h^{-1})	11	0.032	0.023	0.137	0.129	0.227	0.225	0.081	0.077
		±0.048	±0.010	±0.094	±0.046	±0.103	±0.105	±0.048	±0.046

No. sites = number of sites with measurements for each variable. Ave. = average. Adj. = Adjusted.

Table A18. Average metrics across all 13 FLUXNET2015 sites +/- 95% confidence intervals of the means for WFDEI v FN2015 and WFDE5 v FN2015 at 3-hourly time steps (see Appendix tables A9 to A16)

Variable	No. sites	Ave. MBE		Ave. MAE		Ave. Correlation		Ave. Adj. Correlation	
		WFDEI	WFDE5	WFDEI	WFDE5	WFDEI	WFDE5	WFDEI	WFDE5
Tair (°C)	13	0.310	-0.269	2.279	2.169	0.923	0.937	0.762	0.768
		±0.701	±0.982	±0.432	±0.512	±0.060	±0.051	±0.098	±0.069
PSurf (hPa)	10	-3.9	-3.9	9.2	9.0	0.896	0.961	0.421	0.700
		±10.3	±10.2	±8.2	±8.2	±0.098	±0.037	±0.201	±0.213
Qair (kg kg^{-1})	13	0.00060	0.00070	0.00146	0.00121	0.812	0.853	0.167	0.318
		±0.00094	±0.00069	±0.00077	±0.00053	±0.164	±0.139	±0.060	±0.073
Wind (m s^{-1})	13	0.117	-0.094	1.414	1.152	0.525	0.667	0.137	0.435
		±0.689	±0.646	±0.231	±0.334	±0.114	±0.103	±0.076	±0.074
SWdown (W m^{-2})	13	1.926	1.637	48.98	43.604	0.922	0.939	0.881	0.901
		±5.564	±4.338	±9.808	±8.530	±0.020	±0.010	±0.042	±0.023
LWdown (W m^{-2})	8	-10.586	-8.702	20.363	15.522	0.880	0.903	0.542	0.616
		±10.907	±8.905	±4.974	±6.572	±0.093	±0.077	±0.116	±0.109
P. CRU (mm 3h^{-1})	11	0.071	0.082	0.379	0.373	0.210	0.266	0.094	0.172
		±0.031	±0.051	±0.245	±0.247	±0.101	±0.119	±0.064	±0.095
P. GPCC (mm 3h^{-1})	11	0.083	0.071	0.397	0.356	0.182	0.307	0.073	0.197
		±0.050	±0.031	±0.249	±0.241	±0.086	±0.128	±0.063	±0.104

No. sites = number of sites with measurements for each variable. Ave. = average. Adj. = Adjusted.
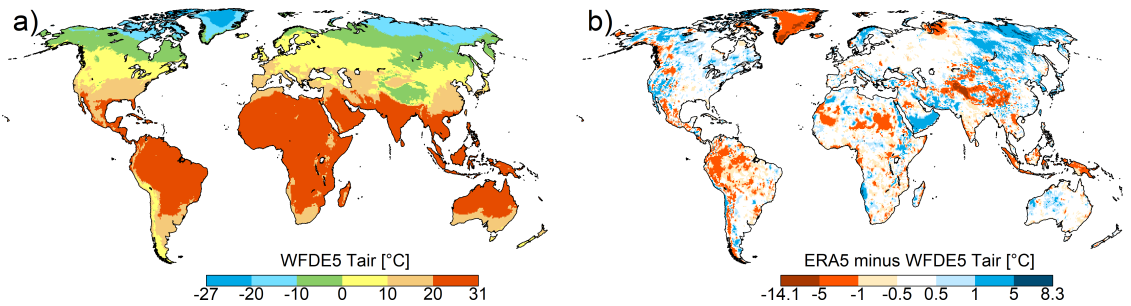
Figure A1. Long-term (1979–2016) average temperature of the climate forcings, displayed as absolute number for WFDE5 (a) and differences to ERA5, computed as ERA5 minus WFDE5 (b). All units in °C.
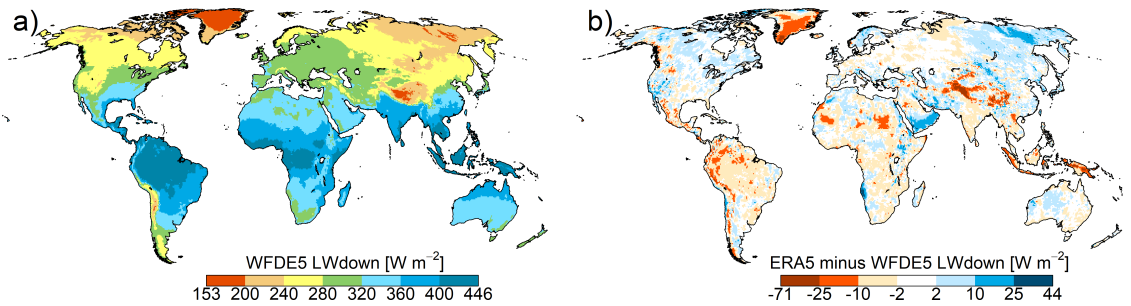
Figure A2. Long-term (1979–2016) average longwave downward radiation of the climate forcings, displayed as absolute number for WFDE5 (a) and differences to ERA5, computed as ERA5 minus WFDE5 (b). All units in W m^{-2}.
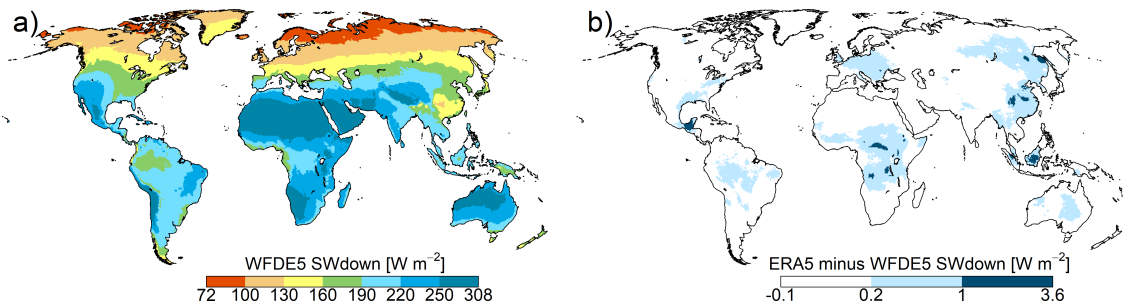
Figure A3. Long-term (1979–2016) average shortwave downward radiation of the climate forcings, displayed as absolute number for WFDE5 (a) and differences to ERA5, computed as ERA5 minus WFDE5 (b). All units in W m^{-2}.

Author contributions. MC implemented the code for the generation of the dataset, led its production and coordinated the paper's writing; GPW advised on the WATCH Forcing Data methodology and on the conversion of his WFDEI FORTRAN code into Python, he ran the validations against FLUXNET2015 site observations and checked the whole paper for consistency and English; AA contributed to the code implementation and to the production of the dataset; NB calculated the aerosol corrections; SL initiated the conversation about bias adjusting ERA5 for impact studies; HMS highlighted the need of bias adjusting ERA5 for hydrological applications at the ISIMIP workshop in Paris (June 2019) and validated the WFDE5 dataset with the global hydrological model WaterGAP; SL and HMS beta tested the WFDE5 dataset; HH provided the description of the ERA5 dataset and was involved in the discussions on the creation of the WFDE5 dataset; CB had the idea of developing WFDE5, put together the team and coordinated the different contributions. All the authors participated in the writing of the present paper, each for their own area of expertise and competence.

Competing interests. The authors declare that they have no conflict of interest.

Acknowledgements. Stefan Lange acknowledges funding from the European Union's Horizon 2020 research and innovation program under grant agreement no. 641816 (CRESCENDO). Hannes Müller Schmied is partly supported by the German Federal Ministry of Education and Research (BMBF, grant no. 01LS1711F). Marco Cucchi acknowledges partial support from the Department of Mathematics and Statistics of the University of Reading. All the authors thanks Stefan Hagemann, Anthony Schrapffer and Xudong Zhou for their thorough and useful reviews of the manuscript. This work used surface meteorological data collected in association with the eddy covariance data acquired and shared by the FLUXNET community, including these networks: AmeriFlux, AfriFlux, AsiaFlux, CarboAfrica, CarboEuropeIP, CarboItaly, CarboMont, ChinaFlux, Fluxnet-Canada, GreenGrass, ICOS, KoFlux, LBA, NECC, OzFlux-TERN, TCOS-Siberia, and USCCC.

370 **References**

Albergel, C., Dutra, E., Munier, S., Calvet, J.-C., Munoz-Sabater, J., de Rosnay, P., and Balsamo, G.: ERA-5 and ERA-Interim driven ISBA land surface model simulations: which one performs better?, Hydrology and Earth System Sciences, 22, 3515–3532, https://doi.org/10.5194/hess-22-3515-2018, https://www.hydrol-earth-syst-sci.net/22/3515/2018/, 2018.

Beck, H. E., Vergopolan, N., Pan, M., Levizzani, V., van Dijk, A. I. J. M., Weedon, G. P., Brocca, L., Pappenberger, F., Huffman, G. J., and
375 Wood, E. F.: Global-scale evaluation of 22 precipitation datasets using gauge observations and hydrological modeling, Hydrology and Earth System Sciences, 21, 6201–6217, https://doi.org/10.5194/hess-21-6201-2017, https://doi.org/10.5194/hess-21-6201-2017, 2017.

Beck, H. E., Pan, M., Roy, T., Weedon, G. P., Pappenberger, F., van Dijk, A. I. J. M., Huffman, G. J., Adler, R. F., and Wood, E. F.: Daily evaluation of 26 precipitation datasets using Stage-IV gauge-radar data for the CONUS, Hydrology and Earth System Sciences, 23, 207–224, https://doi.org/10.5194/hess-23-207-2019, https://www.hydrol-earth-syst-sci.net/23/207/2019/, 2019a.

380 Beck, H. E., Wood, E. F., Pan, M., Fisher, C. K., Miralles, D. G., van Dijk, A. I. J. M., McVicar, T. R., and Adler, R. F.: MSWEP V2 Global 3-Hourly 0.1° Precipitation: Methodology and Quantitative Assessment, Bulletin of the American Meteorological Society, 100, 473–500, https://doi.org/10.1175/BAMS-D-17-0138.1, 2019b.

Becker, A., Finger, P., Meyer-Christoffer, A., Rudolf, B., Schamm, K., Schneider, U., and Ziese, M.: A description of the global land-surface precipitation data products of the Global Precipitation Climatology Centre with sample applications including centennial (trend) analysis
385 from 1901-present, Earth System Science Data, 5, 71–99, https://doi.org/10.5194/essd-5-71-2013, https://www.earth-syst-sci-data.net/5/71/2013/, 2013.

Bellouin, N., Rae, J., Jones, A., Johnson, C., Haywood, J., and Boucher, O.: Aerosol forcing in the Climate Model Intercomparison Project (CMIP5) simulations by HadGEM2-ES and the role of ammonium nitrate, Journal of Geophysical Research: Atmospheres, 116, https://doi.org/10.1029/2011JD016074, https://agupubs.onlinelibrary.wiley.com/doi/abs/10.1029/2011JD016074, 2011.

390 Buck, A. L.: New Equations for Computing Vapor Pressure and Enhancement Factor, Journal of Applied Meteorology, 20, 1527–1532, https://doi.org/10.1175/1520-0450(1981)020<1527:NEFCVP>2.0.CO;2, 1981.

C3S: The Climate Data Store, https://climate.copernicus.eu/climate-data-store, 2020.

C3S: Near surface meteorological variables from 1979 to 2018 derived from bias-corrected reanalysis, CDS, https://doi.org/10.24381/cds.20d54e34, 2020.

395 Chu, H.: FLUXNET2015 dataset release, http://fluxnet.fluxdata.org/2015/12/31/fluxnet2015-dataset-release/, 2015.

Copernicus Climate Change Service: ERA5: Fifth generation of ECMWF atmospheric reanalyses of the global climate, Copernicus Climate Change Service Climate Data Store (CDS), https://cds.climate.copernicus.eu/cdsapp#!/home, 2017.

Dee, D. P., Uppala, S. M., Simmons, A. J., Berrisford, P., Poli, P., Kobayashi, S., Andrae, U., Balmaseda, M. A., Balsamo, G., Bauer, P., Bechtold, P., Beljaars, A. C. M., van de Berg, L., Bidlot, J., Bormann, N., Delsol, C., Dragani, R., Fuentes, M., Geer, A. J., Haim-
400 berger, L., Healy, S. B., Hersbach, H., Hólm, E. V., Isaksen, L., Kållberg, P., Köhler, M., Matricardi, M., McNally, A. P., Monge-Sanz, B. M., Morcrette, J.-J., Park, B.-K., Peubey, C., de Rosnay, P., Tavolato, C., Thépaut, J.-N., and Vitart, F.: The ERA-Interim reanalysis: configuration and performance of the data assimilation system, Quarterly Journal of the Royal Meteorological Society, 137, 553–597, https://doi.org/10.1002/qj.828, https://rmets.onlinelibrary.wiley.com/doi/abs/10.1002/qj.828, 2011.

Döll, P., Kaspar, F., and Lehner, B.: A global hydrological model for deriving water availability indicators: model tuning and valida-
405 tion, Journal of Hydrology, 270, 105–134, https://doi.org/10.1016/S0022-1694(02)00283-4, http://linkinghub.elsevier.com/retrieve/pii/S0022169402002834, 2003.

Ebisuzaki, W.: A Method to Estimate the Statistical Significance of a Correlation When the Data Are Serially Correlated, Journal of Climate, 10, 2147–2153, https://doi.org/10.1175/1520-0442(1997)010<2147:AMTETS>2.0.CO;2, 1997.

Fallah, A., Rakhshandehroo, G. R., Berg, P., O, S., and Orth, R.: Evaluation of precipitation datasets against local observations in southwest-
410 ern Iran, International Journal of Climatology, https://doi.org/10.1002/joc.6445, https://rmets.onlinelibrary.wiley.com/doi/abs/10.1002/joc.6445, 2020.

Frieler, K., Lange, S., Piontek, F., Reyer, C. P. O., Schewe, J., Warszawski, L., Zhao, F., Chini, L., Denvil, S., Emanuel, K., Geiger, T., Halladay, K., Hurtt, G., Mengel, M., Murakami, D., Ostberg, S., Popp, A., Riva, R., Stevanovic, M., Suzuki, T., Volkholz, J., Burke, E., Ciais, P., Ebi, K., Eddy, T. D., Elliott, J., Galbraith, E., Gosling, S. N., Hattermann, F., Hickler, T., Hinkel, J., Hof, C., Huber, V.,
415 Jägermeyr, J., Krysanova, V., Marcé, R., Müller Schmied, H., Mouratiadou, I., Pierson, D., Tittensor, D. P., Vautard, R., van Vliet, M., Biber, M. F., Betts, R. A., Bodirsky, B. L., Deryng, D., Frolking, S., Jones, C. D., Lotze, H. K., Lotze-Campen, H., Sahajpal, R., Thonicke, K., Tian, H., and Yamagata, Y.: Assessing the impacts of 1.5 °C global warming – simulation protocol of the Inter-Sectoral Impact Model Intercomparison Project (ISIMIP2b), Geoscientific Model Development, 10, 4321–4345, https://doi.org/10.5194/gmd-10-4321-2017, 2017.

420 Haddeland, I., Clark, D. B., Franssen, W., Ludwig, F., Voß, F., Arnell, N. W., Bertrand, N., Best, M., Folwell, S., Gerten, D., Gomes, S., Gosling, S. N., Hagemann, S., Hanasaki, N., Harding, R., Heinke, J., Kabat, P., Koirala, S., Oki, T., Polcher, J., Stacke, T., Viterbo, P., Weedon, G. P., and Yeh, P.: Multimodel Estimate of the Global Terrestrial Water Balance: Setup and First Results, Journal of Hydrometeorology, 12, 869–884, https://doi.org/10.1175/2011JHM1324.1, 2011.

Hagemann, S., Chen, C., Haerter, J. O., Heinke, J., Gerten, D., and Piani, C.: Impact of a Statistical Bias Correction on the Pro-
425 jected Hydrological Changes Obtained from Three GCMs and Two Hydrology Models, Journal of Hydrometeorology, 12, 556–578, https://doi.org/10.1175/2011JHM1336.1, 2011.

Harris, I., Osborn, T. J., Jones, P., and Lister, D.: Version 4 of the CRU TS monthly high-resolution gridded multivariate climate dataset, Scientific Data, 7, https://doi.org/10.1038/s41597-020-0453-3, https://doi.org/10.1038/s41597-020-0453-3, 2020.

Hempel, S., Frieler, K., Warszawski, L., Schewe, J., and Piontek, F.: A trend-preserving bias correction – the ISI-MIP approach, Earth System
430 Dynamics, 4, 219–236, https://doi.org/10.5194/esd-4-219-2013, 2013.

Hersbach, H., Peubey, C., Simmons, A., Berrisford, P., Poli, P., and Dee, D.: ERA-20CM: A twentieth-century atmospheric model ensemble, Quart. J. Roy. Meteorol. Soc., 141, 2350–2375, 2015.

Hersbach, H., Bell, W., Berrisford, P., Horányi, A., J., M.-S., Nicolas, J., Radu, R., Schepers, D., Simmons, A., Soci, C., and Dee, D.: Global reanalysis: goodbye ERA-Interim, hello ERA5, https://doi.org/10.21957/VF291HEHD7, https://www.ecmwf.int/node/19027, 2019.

435 Hersbach, H., Bell, B., Berrisford, P., Hirahara, S., Horányi, A., Muñoz-Sabater, J., Nicolas, J., Peubey, C., Radu, R., Schepers, D., Simmons, A., Soci, C., Abdalla, S., Abellan, X., Balsamo, G., Bechtold, P., Biavati, G., Bidlot, J., Bonavita, M., Chiara, G., Dahlgren, P., Dee, D., Diamantakis, M., Dragani, R., Flemming, J., Forbes, R., Fuentes, M., Geer, A., Haimberger, L., Healy, S., Hogan, R. J., Hólm, E., Janisková, M., Keeley, S., Laloyaux, P., Lopez, P., Lupu, C., Radnoti, G., Rosnay, P., Rozum, I., Vamborg, F., Villaume, S., and Thépaut, J.-N.: The ERA5 global reanalysis, Quarterly Journal of the Royal Meteorological Society, https://doi.org/10.1002/qj.3803,
440 https://doi.org/10.1002/qj.3803, 2020.

Hirahara, S., Alonso-Balmaseda, M., de Boisseson, E., and Hersbach, H.: Sea Surface Temperature and Sea Ice Concentration for ERA5, https://www.ecmwf.int/node/16555, 2016.

Inness, A., Ades, M., Agustí-Panareda, A., Barré, J., Benedictow, A., Blechschmidt, A.-M., Dominguez, J. J., Engelen, R., Eskes, H., Flem-ming, J., Huijnen, V., Jones, L., Kipling, Z., Massart, S., Parrington, M., Peuch, V.-H., Razinger, M., Remy, S., Schulz, M., and Suttie, M.:

445   The CAMS reanalysis of atmospheric composition, Atmospheric Chemistry and Physics, 19, 3515–3556, https://doi.org/10.5194/acp-19-3515-2019, https://www.atmos-chem-phys.net/19/3515/2019/, 2019.

Jones, P. W.: First- and Second-Order Conservative Remapping Schemes for Grids in Spherical Coordinates, Monthly Weather Review, 127, 2204–2210, https://doi.org/10.1175/1520-0493(1999)127<2204:FASOCR>2.0.CO;2, 1999.

Lange, S.: Bias correction of surface downwelling longwave and shortwave radiation for the EWEMBI dataset, Earth System Dynamics, 9,
450   627–645, https://doi.org/10.5194/esd-9-627-2018, 2018.

Lange, S.: EartH2Observe, WFDEI and ERA-Interim data Merged and Bias-corrected for ISIMIP (EWEMBI), https://doi.org/10.5880/pik.2019.004, 2019a.

Lange, S.: Trend-preserving bias adjustment and statistical downscaling with ISIMIP3BASD (v1.0), Geoscientific Model Development, 12, 3055–3070, https://doi.org/10.5194/gmd-12-3055-2019, 2019b.

455   Lange, S.: WFDE5 over land merged with ERA5 over the ocean (W5E5), https://doi.org/10.5880/pik.2019.023, 2019c.

Lange, S.: ISIMIP3BASD v2.4.1, https://doi.org/10.5281/zenodo.3898426, 2020.

Müller Schmied, H., Eisner, S., Franz, D., Wattenbach, M., Portmann, F. T., Flörke, M., and Döll, P.: Sensitivity of simulated global-scale freshwater fluxes and storages to input data, hydrological model structure, human water use and calibration, Hydrology and Earth System Sciences, 18, 3511–3538, https://doi.org/10.5194/hess-18-3511-2014, http://www.hydrol-earth-syst-sci-discuss.net/11/1583/2014/, 2014.

460   Müller Schmied, H., Adam, L., Eisner, S., Fink, G., Flörke, M., Kim, H., Oki, T., Portmann, F. T., Reinecke, R., Riedel, C., Song, Q., Zhang, J., and Döll, P.: Variations of global and continental water balance components as impacted by climate forcing uncertainty and human water use, Hydrology and Earth System Sciences, 20, 2877–2898, https://doi.org/10.5194/hess-20-2877-2016, http://www.hydrol-earth-syst-sci.net/20/2877/2016/, 2016.

Nash, J. and Sutcliffe, J.: River flow forecasting through conceptual models part I — A discussion of principles, Journal of Hydrology, 10,
465   282–290, https://doi.org/10.1016/0022-1694(70)90255-6, http://www.sciencedirect.com/science/article/pii/0022169470902556, 1970.

New, M., Hulme, M., and Jones, P.: Representing Twentieth-Century Space–Time Climate Variability. Part I: Development of a 1961–90 Mean Monthly Terrestrial Climatology, Journal of Climate, 12, 829–856, https://doi.org/10.1175/1520-0442(1999)012<0829:RTCSTC>2.0.CO;2, 1999.

New, M., Hulme, M., and Jones, P.: Representing Twentieth-Century Space–Time Climate Variability. Part II: Development
470   of 1901–96 Monthly Grids of Terrestrial Surface Climate, Journal of Climate, 13, 2217–2238, https://doi.org/10.1175/1520-0442(2000)013<2217:RTCSTC>2.0.CO;2, 2000.

Pastorello, G. Z., Papale, D., Chu, H., Trotta, C., Agarwal, D. A., Canfora, E., Baldocchi, D. D., and Torn, M. S.: A new data set to keep a sharper eye on land-air exchanges, Eos, 98, https://doi.org/10.1029/2017EO071597, 2017.

Sato, M., Hansen, J. E., McCormick, M. P., and Pollack, J. B.: Stratospheric aerosol optical depths, 1850–1990, Journal of Geophysical
475   Research: Atmospheres, 98, 22 987–22 994, https://doi.org/10.1029/93JD02553, https://agupubs.onlinelibrary.wiley.com/doi/abs/10.1029/93JD02553, 1993.

Schneider, U., Becker, A., Finger, P., Meyer-Christoffer, A., Ziese, M., and Rudolf, B.: GPCC's new land surface precipitation climatology based on quality-controlled in situ data and its role in quantifying the global water cycle, Theoretical and Applied Climatology, 115, 15–40, https://doi.org/10.1007/s00704-013-0860-x, 2014.

480   Schneider, U., Becker, A., Finger, P., Meyer-Christoffer, A., and Ziese, M.: GPCC Full Data Monthly Product Version 2018 at 0.5°: Monthly Land-Surface Precipitation from Rain-Gauges built on GTS-based and Historical Data, https://doi.org/10.5676/DWD_GPCC/FD_M_V2018_050, 2018.

Sheffield, J., Goteti, G., and Wood, E. F.: Development of a 50-Year High-Resolution Global Dataset of Meteorological Forcings for Land Surface Modeling, Journal of Climate, 19, 3088–3111, https://doi.org/10.1175/JCLI3790.1, 2006.

485 Thomason, L. W., Ernest, N., Millán, L., Rieger, L., Bourassa, A., Vernier, J.-P., Manney, G., Luo, B., Arfeuille, F., and Peter, T.: A global space-based stratospheric aerosol climatology: 1979–2016, Earth System Science Data, 10, 469–492, https://doi.org/10.5194/essd-10-469-2018, https://www.earth-syst-sci-data.net/10/469/2018/, 2018.

Uppala, S. M., Kållberg, P. W., Simmons, A. J., Andrae, U., Bechtold, V. D. C., Fiorino, M., Gibson, J. K., Haseler, J., Hernandez, A., Kelly,
490 G. A., Li, X., Onogi, K., Saarinen, S., Sokka, N., Allan, R. P., Andersson, E., Arpe, K., Balmaseda, M. A., Beljaars, A. C. M., Berg, L. V. D., Bidlot, J., Bormann, N., Caires, S., Chevallier, F., Dethof, A., Dragosavac, M., Fisher, M., Fuentes, M., Hagemann, S., Hólm, E., Hoskins, B. J., Isaksen, L., Janssen, P. A. E. M., Jenne, R., Mcnally, A. P., Mahfouf, J.-F., Morcrette, J.-J., Rayner, N. A., Saunders, R. W., Simon, P., Sterl, A., Trenberth, K. E., Untch, A., Vasiljevic, D., Viterbo, P., and Woollen, J.: The ERA-40 re-analysis, Quarterly Journal of the Royal Meteorological Society, 131, 2961–3012, https://doi.org/10.1256/qj.04.176, https://rmets.onlinelibrary.wiley.com/doi/abs/10.
495 1256/qj.04.176, 2005.

Warszawski, L., Frieler, K., Huber, V., Piontek, F., Serdeczny, O., and Schewe, J.: The Inter-Sectoral Impact Model Intercomparison Project (ISI-MIP): Project framework, Proceedings of the National Academy of Sciences, 111, 3228–3232, https://doi.org/10.1073/pnas.1312330110, 2014.

Weedon, G. P., Gomes, S., Viterbo, P., Österle, H., Adam, J. C., Bellouin, N., Boucher, O., and Best, M.: The WATCH Forcing Data
500 1958–2001: A meteorological forcing dataset for land surface- and hydrological-models, Tech. rep., WATCH Technical Report 22, http://www.eu-watch.org/publications/technical-reports, 2010.

Weedon, G. P., Gomes, S., Viterbo, P., Shuttleworth, W. J., Blyth, E., Österle, H., Adam, J. C., Bellouin, N., Boucher, O., and Best, M.: Creation of the WATCH Forcing Data and Its Use to Assess Global and Regional Reference Crop Evaporation over Land during the Twentieth Century, Journal of Hydrometeorology, 12, 823–848, https://doi.org/10.1175/2011JHM1369.1, 2011.

505 Weedon, G. P., Balsamo, G., Bellouin, N., Gomes, S., Best, M. J., and Viterbo, P.: The WFDEI meteorological forcing data set: WATCH Forcing Data methodology applied to ERA-Interim reanalysis data, Water Resources Research, 50, 7505–7514, https://doi.org/10.1002/2014WR015638, 2014.

Willmott, C. J. and Matsuura, K.: Advantages of the mean absolute error (MAE) over the root mean square error (RMSE) in assessing average model performance, Climate Research, 30, 79–82, https://doi.org/10.3354/cr030079, 2005.

510 Zscheischler, J., Fischer, E. M., and Lange, S.: The effect of univariate bias adjustment on multivariate hazard estimates, Earth System Dynamics, 10, 31–43, https://doi.org/10.5194/esd-10-31-2019, 2019.